Hirzebruch surfaces, Tyurin degenerations and toric mirrors: bridging generalized Calabi-Yau constructions

PER BERGLUND AND TRISTAN HÜBSCH

There is a large number of different ways of constructing Calabi-Yau manifolds, as well as related non-geometric formulations, relevant in string compactifications. Showcasing this diversity, we discuss explicit deformation families of discretely distinct Hirzebruch hypersurfaces in $\mathbb{P}^n \times \mathbb{P}^1$ and identify their toric counterparts in detail. This precise isomorphism is then used to investigate some of their special divisors of interest, and in particular the secondary deformation family of their Calabi-Yau subspaces. Moreover, most of the above so called Hirzebruch scrolls are non-Fano, and their (regular) Calabi-Yau hypersurfaces are Tyurin-degenerate, but admit novel (Laurent) deformations by special rational sections as well as a sweeping generalization of the *transposition construction* of mirror models. This bi-projective embedding also reveals a novel deformation connection between distinct toric spaces, and so also the various divisors of interest including their Calabi-Yau subspaces.

1. Introduction, rationale and summary

Constructing complex algebraic varieties as complete intersections of holomorphic hypersurfaces within a well-understood "ambient" space, A, has recently been generalized so as to include cases where some of those hypersurfaces have a negative degree over some factors in A [1]. The diffeomorphism class and cohomology of such *generalized complete intersections* (gCI, gCICY if $c_1 = 0$) have been studied [2, 3], and they were soon provided with a rigorous scheme-theoretic definition [4]. Such constructions of immediate physics interest are anticanonical (Calabi-Yau) hypersurfaces in non-Fano varieties, their toric models and their Laurent deformations were further explored in [5], extending the already immense database [6] to include infinitely many, though not necessarily distinct, constructions.

   The purpose of this article, in part, is to provide a bridge between these different approaches, aiming to further explore the generalization [5] of the transposition mirror model construction [7–9] and Batyrev's toric construction [10]; see also [11] and references therein. To this end, we follow suit from the earlier work [2, 5] and continue to examine the generalized complete intersection Calabi-Yau models in the "proof of concept" showcasing the infinite sequence of deformation families $\left[\begin{smallmatrix}\mathbb{P}^n\\\mathbb{P}^1\end{smallmatrix}\middle\|\begin{smallmatrix}1\\m\end{smallmatrix}\middle|\begin{smallmatrix}n\\2-m\end{smallmatrix}\right]$ and their toric rendition. The bi-projective embedding is the (*generalized* when $m \geqslant 3$) complete intersection of two hypersurfaces of bi-degrees $\binom{1}{m}$ and $\binom{n}{2-m}$, were the latter hypersurface is for $m \geqslant 3$ well defined *only within* the former. This *ordered* approach reveals a detailed structure in this deformation family of Calabi-Yau models.

   In particular, we first focus on the deformation families $\left[\begin{smallmatrix}\mathbb{P}^n\\\mathbb{P}^1\end{smallmatrix}\middle\|\begin{smallmatrix}1\\m\end{smallmatrix}\right]$ of Hirzebruch scrolls, and provide explicit, coordinate-level isomorphisms between such hypersurfaces [2, 12] and their toric rendition [5]; see also [13–15]. This naturally maps their cohomology data, as well as their special subspaces of interest, including the hallmark divisor of maximally negative self-intersection (dubbed *directrix* [16]), and then also their Calabi-Yau subspaces, as detailed in §2. The remainder of that section shows that the deformation family of Hirzebruch scrolls, $\left[\begin{smallmatrix}\mathbb{P}^n\\\mathbb{P}^1\end{smallmatrix}\middle\|\begin{smallmatrix}1\\m\end{smallmatrix}\right]$, contains besides the *central* $F_{m;0}^{(n)}$ also a hierarchy of its diffeomorphic but *discretely different* complex deformations, $F_{m;\vec{\epsilon}}^{(n)}$, each harboring less negative (sub-)directrices. This extends our comparisons across a detailed web of bi-projective and toric constructions — both the infinite hierarchy of Hirzebruch scrolls, and then also their Calabi-Yau subspaces.

   Section 3 shows that the regular Calabi-Yau hypersurfaces, $X_m^{(n-1)} \subset F_{m;0}^{(n)}$, are for $m \geqslant 3$ always Tyurin-degenerate, their codimension-1

singularity itself Calabi-Yau. While generic scrolls $F_{m;\vec{\epsilon}}^{(n)}$ admit smoothing such hypersurfaces by regular sections, those in the central $F_{m;0}^{(n)}$ can only be desingularized by Laurent deformations [5]. The latter require special attention to the putative pole singularities, detailed in §3.2, but are shown in §§3.3–3.4 to admit a straightforward extension of the transposition mirror model construction [5, 7]. Finally, §3.5 discusses such Laurent deformations as *virtual varieties* (Weil divisors), as well as a recasting in terms of desingularized finite quotients of ramified multiple covers.

The inclusion of these ideas and results in the gauged linear sigma models (GLSMs) [17, 18] are discussed in §4, and our concluding remarks are collected in §5. The technically more detailed material is deferred to the appendices. As indicated throughout, the results presented herein indicate several avenues for further study, the pursuit of which is however beyond the scope of such a "proof of concept" article.

2. Hirzebruch scrolls

Following Hirzebruch's original definition [12], we identify the particular hypersurface

$$
(2.1) \qquad F_{m;0}^{(n)} := \left\{ p_0(x,y) = 0 \right\} \in \begin{bmatrix} \mathbb{P}^n \\ \mathbb{P}^1 \end{bmatrix} \begin{Vmatrix} 1 \\ m \end{Vmatrix},
$$

$$
p_0(x,y) := x_0 {y_0}^m + x_1 {y_1}^m
$$

as the *central* member of the deformation family of degree-$\binom{1}{m}$ hypersurfaces in $\mathbb{P}^n \times \mathbb{P}^1$:

$$
F_{m;\epsilon}^{(n)} := \left\{ p_{\vec{\epsilon}}(x,y)=0 \right\} \in \begin{bmatrix} \mathbb{P}^n \\ \mathbb{P}^1 \end{bmatrix} \begin{Vmatrix} 1 \\ m \end{Vmatrix},
$$

$$
(2.2) \qquad p_{\vec{\epsilon}}(x,y) := p_0(x,y) + \sum_{a=0}^{n} \sum_{\ell=1}^{m-1} \epsilon_{a\ell}\, x_a\, {y_0}^{m-\ell} {y_1}^{\ell},
$$

explicitly (and coarsely) parametrized by the $\epsilon_{a\ell} \in \mathbb{C}$. The gradient $\partial p_0 = ({y_0}^m, {y_1}^m, \dots)$ of even the central model (2.1) cannot vanish anywhere on $\mathbb{P}^1$ since y_0, y_1 cannot both vanish: even $p_0(x,y)$ is *transverse* (basepoint free), so $F_{m;0}^{(n)} := p_0^{-1}(0)$ is nonsingular, not just the generic $F_{m;\epsilon}^{(n)} := p_\epsilon^{-1}(0)$. Again following Hirzebruch [12], we identify $F_{m;0}^{(n)}$ also with the m-twisted $\mathbb{P}^{n-1}$-bundle over $\mathbb{P}^1$ as well as the projectivization $\mathbb{P}\big(\mathcal{O}_{\mathbb{P}^1} \oplus \mathcal{O}_{\mathbb{P}^1}(m)^{\oplus(n-1)}\big)$.

A key feature of deformation families such as (2.2) is that although the smooth hypersurfaces in the families with a fixed $m \simeq m \,(\mathrm{mod}\, n)$ are

all diffeomorphic to each other, they form a *discrete* collection of distinct complex manifolds — and these distinctions also pertain to the Calabi-Yau hypersurfaces therein.

2.1. Topological characteristics

As usual, $H^r(F_m^{(n)}, \mathbb{Z}) = H^r(\mathbb{P}^n \times \mathbb{P}^1, \mathbb{Z})$ without torsion [2], and with J_1^{n+1}, J_2^2, $J_1^n J_2 = 0$,

$$(2.3) \quad c(F_m^{(n)}) = \frac{(1+J_1)^{n+1}(1+J_2)^2}{1+J_1+mJ_2} = (1+J_1-mJ_2)(1+J_1)^{n-1}(1+J_2)^2.$$

The simplification owes to the identity $\frac{(1+J_1)^2}{1+J_1+mJ_2} = (1+J_1-mJ_2)$ insured by the nilpotence of J_2. Standard (Bézout's theorem) computations then provide the n-tuple intersection numbers [19]:

$$(2.4) \quad \begin{aligned} [J_1^n] &= \begin{bmatrix} \mathbb{P}^n & 1 & 1 & \cdots & 1 \\ \mathbb{P}^1 & m & 0 & \cdots & 0 \end{bmatrix} = m, \\ [J_1^{n-1}J_2] &= \begin{bmatrix} \mathbb{P}^n & 1 & 1 & \cdots & 1 & 0 \\ \mathbb{P}^1 & m & 0 & \cdots & 0 & 1 \end{bmatrix} = 1, \end{aligned}$$

and all other intersections vanish again owing to $J_2^2 = 0$. Also, powers of (aJ_1+bJ_2) may be evaluated against complementary Chern classes to yield, e.g., for $n=4$:

$$(2.5a) \quad \begin{aligned} C_1{}^3[aJ_1+bJ_2] &= 16[6a + (\underline{4b+ma})], \\ C_1{\cdot}C_2[aJ_1+bJ_2] &= 2[22a + 3(\underline{4b+ma})], \end{aligned}$$

$$(2.5b) \quad \begin{aligned} C_3[aJ_1+bJ_2] &= 12a + (\underline{4b+ma}), \\ C_1{}^2[(aJ_1+bJ_2)^2] &= 8a[2a + (\underline{4b+ma})], \end{aligned}$$

$$(2.5c) \quad \begin{aligned} C_2[(aJ_1+bJ_2)^2] &= a(8a + 3(\underline{4b+ma})], \\ C_1[(aJ_1+bJ_2)^3] &= a^2(2a + 3(\underline{4b+ma})). \end{aligned}$$

Finally, the Chern *numbers* are m-independent:

$$(2.5d) \quad \begin{aligned} C_1{}^4 &= 512, \quad C_1{}^2{\cdot}C_2 = 224, \\ C_1{\cdot}C_3 &= 56, \quad C_2{}^2 = 96, \quad C_4 = \chi_E = 8. \end{aligned}$$

Jointly, (2.5) indicate an $[m \,(\mathrm{mod}\, n)]$-dependence of these topological invariants for $n=4$, verified by the integral basis change, $\widetilde{J}_1 := J_1 - kJ_2$ and

$\widetilde{J}_2 := J_2$:

$$(2.6) \qquad [\widetilde{J}_1^n] = (m-kn) \qquad \text{and} \qquad [\widetilde{J}_1^{n-1}\widetilde{J}_2] = 1, \qquad k \in \mathbb{Z},$$

This implies that $F_m^{(n)} \approx_{\mathbb{R}} F_{m-kn}^{(n)}$ for integral k are all diffeomorphic to each other [20]: they are the same real manifold, and so are then the Calabi-Yau hypersurfaces, $X_m^{(n-1)} \approx_{\mathbb{R}} X_{m-kn}^{(n-1)} \in F_m^{(n)}[c_1]$; for details, see [2].

The entire infinite m-sequence of deformation families of hypersurfaces (2.2) thus harbors precisely n distinct real manifolds, distinguished only by $[m \pmod n]$. In particular, all transverse (and so smooth) scrolls in the deformation families $\left[\mathbb{P}^n \middle\| \begin{smallmatrix}1\\m\end{smallmatrix}\right]$ for any fixed $m \simeq m \pmod n$ are the same real manifold.

2.2. Holomorphic characteristics

The m-sequence of deformation families of hypersurfaces (2.2) however admits infinitely many *complex* manifolds, distinguished by m, unreduced: The hallmark *holomorphic* characteristic of Hirzebruch's original [12, 21], $F_m^{(2)} = F_m^{(2)} := \mathbb{P}(\mathcal{O} \oplus \mathcal{O}(m))$, is its exceptional irreducible curve, S_m, a holomorphic hypersurface of self-intersection $-m$, the *directrix* [16, p. 525]. Correspondingly, each Hirzebruch n-fold $F_m^{(n)}$ contains an *exceptional* irreducible (holomorphic) hypersurface $S_m \subset_{\mathbb{C}} F_m^{(n)}$ of self-intersection $-(n-1)m$. Additional relevant holomorphic distinctions are discussed in Appendix A, including the result

$$(2.7a) \qquad \dim H^0(F_m^{(n)}, T) = n^2 + 2 + \Delta_m^{(n)} \quad \text{and} \quad \dim H^1(F_m^{(n)}, T) = \Delta_m^{(n)},$$

where the number of exceptional contributions is, using the step-function $\vartheta_a^b := \{1 \text{ if } a \leqslant b, \ 0 \text{ otherwise}\}$:

$$(2.7b) \quad \Delta_{m;0}^{(n)} = \vartheta_1^m (n-1)(m-1), \quad \text{for } F_{m,0}^{(n)} = \{x_0\, y_0^m + x_1\, y_1^m = 0\} \in \left[\mathbb{P}^n \middle\| \begin{smallmatrix}1\\m\end{smallmatrix}\right],$$

$$(2.7c) \quad \Delta_{m;\epsilon \neq 0}^{(n)} < \Delta_{m;0}^{(n)}; \quad \text{for generic cases, } \Delta_{m;\epsilon \neq 0}^{(n)} = 0.$$

As there always exist more local reparametrizations than local deformations of the complex structure, $\dim H^0(F_m^{(n)}, T) > \dim H^1(F_m^{(n)}, T)$, the scrolls $F_m^{(n)}$ are effectively rigid: their space of complex structure deformations modulo reparametrizations is discrete [2].

This "jumping" (2.7) in the dimensions of $H^*(F_{m;\epsilon}^{(n)}, T)$ depending on the concrete choice of the defining equation (2.1)–(2.2) again illustrates the variability of complex manifolds provided by even a simple deformation family such as $\left[\mathbb{P}^n \middle\| \begin{smallmatrix}1\\m\end{smallmatrix}\right]$. Even the simplest $(F_2^{(2)} \rightsquigarrow F_0^{(2)}$, see [22] and [19, §3.1.2])

of such discrete deformations has been known to affect string compactifications [23, 24]. Another, phenomenologically relevant effect of such discrete deformations was explored in [25–27].

The directrix. The homology class of the directrix is easy to represent as $[S_m] = [J_1] - [mJ_2]$, so indeed

$$(2.8) \qquad [S_m]^n = \begin{bmatrix} \mathbb{P}^n \\ \mathbb{P}^1 \end{bmatrix} \begin{vmatrix} 1 \\ m \end{vmatrix} \begin{matrix} 1 & \cdots & 1 \\ -m & \cdots & -m \end{matrix} = m + n(-m) = -(n-1)m.$$

An *irreducible* holomorphic submanifold representative of $[S_m]$ must be the zero-locus of a degree-$\binom{1}{-m}$ global holomorphic section. No such section exist on $A = \mathbb{P}^n \times \mathbb{P}^1$, but there *does* exist a unique such section on $F_m^{(n)} = F_{m;0}^{(n)}$ and is easily constructed following the techniques introduced in [1, 2, 4]. To highlight the novelty and more general uses of this explicit construction, we adapt from [2]: The key point is to identify sections $\mathfrak{s}(x,y)$ on the zero-locus $\{p_{\vec{\epsilon}} = 0\} \subset A$ with the restriction of the *equivalence class* of sections[1], $[\mathfrak{s}(x,y) \,(\mathrm{mod}\, p_{\vec{\epsilon}})]$, on all of A. For example, a total degree-$\binom{1}{-m}$ multiple of $p_0(x,y)$ is of the form

$$(2.9) \qquad \frac{p_0(x,y)}{(y_0\,y_1)^m} = \left(\frac{x_0}{y_1^m} + \frac{x_1}{y_0^m} \right), \qquad \deg = \binom{1}{-m},$$

which serves as the $r_0 = r_1 = m$ case of the more general:

Construction 1. *Given a degree-$\binom{1}{m}$ hypersurface $\{p_{\vec{\epsilon}}(x,y)\,0\} \subset \mathbb{P}^n \times \mathbb{P}^1$ as in (2.2), construct*
$$(2.10)$$
$$\deg = \binom{1}{m - r_0 - r_1}: \quad \mathfrak{s}_{\vec{\epsilon}}(x,y;\lambda) := \operatorname*{Flip}_{y_0} \left[\frac{1}{y_0^{r_0}\, y_1^{r_1}} p_{\vec{\epsilon}}(x,y) \right] (\mathrm{mod}\, p_{\vec{\epsilon}}(x,y)),$$

progressively decreasing $r_0 + r_1 = 2m, 2m-1, \cdots$, and keeping only those Laurent polynomials that contain both y_0- and y_1-denominators but no y_0, y_1-mixed ones. The "Flip_{y_i}" operator changes the relative sign of the rational monomials with y_i-denominators. For algebraically independent such sections, restrict to a subset with maximally negative degrees that are not overall (y_0, y_1)-multiples of each other.

---

[1]In physics, gauge potentials are a prime example, being defined only up to gauge transformations: $A_\mu \simeq A_\mu + \partial_\mu \lambda$. This enables the Wu-Yang construction of a magnetic monopole [28].

In particular, the $r_0 = r_1 = m$ and $p_0(x,y) = \lim_{\vec{\epsilon} \to 0} p_{\vec{\epsilon}}(x,y)$ case produces the degree-$\left(\begin{smallmatrix} 1 \\ -m \end{smallmatrix} \right)$ directrix:

$$(2.11) \qquad \mathfrak{s}(x,y) = \mathfrak{s}_0(x,y) = \left[\left(\frac{x_0}{y_1{}^m} - \frac{x_1}{y_0{}^m} \right) + \frac{\lambda}{(y_0\, y_1)^m} p_0(x,y) \right]$$
$$= \begin{cases} +2\frac{x_0}{y_1{}^m} & \text{if } y_1 \neq 0, \quad \lambda = +1, \\ -2\frac{x_1}{y_0{}^m} & \text{if } y_0 \neq 0, \quad \lambda = -1. \end{cases}$$

Designed to generalize this patch-wise feature, the mod-$p_{\vec{\epsilon}}$ equivalence class of sections has a well-defined and holomorphic local representative everywhere on A. Since the difference $\mathfrak{s}_{\vec{\epsilon}}(x,y;\lambda) - \mathfrak{s}_{\vec{\epsilon}}(x,y;\lambda')$ vanishes where $p_{\vec{\epsilon}}(x,y) = 0$, the two local representatives such as (2.11) define a single well-defined holomorphic section (2.10) on the zero-locus $F_{m;\vec{\epsilon}}^{(n)} := \{p_{\vec{\epsilon}}(x,y) = 0\}$. Moreover, $\partial \mathfrak{s}_0 = \left(\frac{1}{y_1{}^m}, -\frac{1}{y_0{}^m}, \dots \right)$ cannot vanish anywhere on $\mathbb{P}^1$ since $y_0, y_1 < \infty$; the analogous is true of $\mathfrak{s}_{\vec{\epsilon}}(x,y)$ for generic $\vec{\epsilon}$. The section $\mathfrak{s}_{\vec{\epsilon}}(x,y)|_{F_{m;\vec{\epsilon}}^{(n)}}$ is thereby transverse (basepoint free) and the holomorphic hypersurface $\left(S_{m;\vec{\epsilon}} := \mathfrak{s}_{\vec{\epsilon}}^{-1}(0) \right) \subset F_{m;\vec{\epsilon}}^{(n)}$ is nonsingular and so irreducible. Away from $\{p_{\vec{\epsilon}}(x,y) = 0\}$, $\mathfrak{s}_{\vec{\epsilon}}(x,y)$ can only define an equivalence class of subspaces corresponding to $[S_{m;\vec{\epsilon}}] \in H_*(A)$. If $r_0 = r_1$ and $p_{\vec{\epsilon}}(x,y)$ is $y_0 \leftrightarrow y_1$ symmetric, Flip_{y_0} evidently flips the sign in $p_{\vec{\epsilon}}(x,y)$ itself, but not so more generally; see § 2.5 for examples.

The Czech cohomology framework was explicitly shown to provide such constructions with a rigorous scheme-theoretic definition [4]. Technically, the putative poles in (2.11) are evaded by clearing the denominators and connecting the patch-wise defined sections by the Mayer-Vietoris sequence. Reassured by the existence of this formal-foundational framework, here we continue the analysis following [2, 5]. Also, the toric framework reached in the next subsection will reveal that these technical complexities are not intrinsic, but a property of the embedding.

It should be clear that mod-$p_{\vec{\epsilon}}$ equivalence classes of sections more negative than (2.10) cannot have a well-defined holomorphic representative everywhere on A. In turn, any multiple of $\mathfrak{s}_{\vec{\epsilon}}(x,y)$ by a regular x,y-polynomial is also a holomorphic mod-$p_{\vec{\epsilon}}$ equivalence class of sections, of a correspondingly less negative degree, but is clearly not algebraically independent.

2.3. Toric rendition

Let's focus first on the central, $\vec{\epsilon}=0$ case, where the explicitly complementary form of (2.1) and (2.11) suggests the reparametrization

(2.12a)
$$(x_0, x_1, x_2, \cdots ; y_0, y_1) \rightarrow (\, p_0\, ,\, \mathfrak{s}\, ,\, x_2, \cdots ; y_0, y_1),$$
$$\det\left[\frac{\partial(\, p_0\, ,\, \mathfrak{s}\, ,\, x_2, \cdots ; y_0, y_1)}{\partial(x_0, x_1, x_2, \cdots ; y_0, y_1)}\right] = -2,$$

which leaves the $p_0=0$ hypersurface parametrized by $(\mathfrak{s}, x_2, \cdots ; y_0, y_1)$. The new variables inherit the $\mathbb{P}^n\times\mathbb{P}^1$ degrees, and are identified with the Cox variables of the toric rendition of $F_m^{(n)}$ as given in [5]:

(2.12b)

	x_0	x_1	x_2	$\cdots$	x_n	y_0	y_1			p_0	$\mathfrak{s}$	x_2	$\cdots$	x_n	y_0	y_1
$\mathbb{P}^n$	1	1	1	$\cdots$	1	0	0	$\xrightarrow{(2.12a)}$		1	1	1	$\cdots$	1	0	0
$\mathbb{P}^1$	0	0	0	$\cdots$	0	1	1			m	$-m$	0	$\cdots$	0	1	1

		X_1	X_2	$\cdots$	X_n	X_{n+1}	X_{n+2}
$\xrightarrow{p_0=0}$		1	1	$\cdots$	1	0	0
		$-m$	0	$\cdots$	0	1	1

The $\mathbb{P}^n\times\mathbb{P}^1$-inherited degrees form the Mori vectors (given in the rows of the right-hand side tabulation), i.e., the GLSM gauge charges [17, 18], $Q_i^a := Q^a(X_i)$: $Q^1 = (1, 1, \cdots, 1, 0, 0)$ and $Q^2 = (-m, 0, \cdots, 0, 1, 1)$.

The n-space orthogonal to these two $(n+2)$-vectors is spanned by n integral $(n+2)$-vectors ν_i^κ (with $\kappa=1,\ldots,n$ and $i=1,\ldots,n+2$), a choice of which is shown in the upper n rows:

(2.13)

In turn, the *columns* in the tabulation (2.13) specify: (**1**) Below the divide are the 2-vector generators, $\vec{Q}_i$, of the secondary fan, shown at right in (2.13) for $n=3$ and $m=4$. (**2**) Above the horizontal divide are the n-vector generators, $\vec{\nu}_i \ll \Sigma_{F_m^{(n)}}$, of the (primary) fan defining the toric variety $F_m^{(n)}$. The so-called *spanning polytope* [14], $\Delta^\star_{F_m^{(n)}}$, is shown at left: its faces are the bases of the cones in $\Sigma_{F_m^{(n)}}$, denoted "$\Delta^\star_{F_m^{(n)}} \gg \Sigma_{F_m^{(n)}}$." For $m\geqslant 3$, $\Delta^\star_{F_m^{(n)}}$ is non-convex (ν_1

is a saddle-point), reflecting that $F_m^{(n)}$ not Fano. This fan also shows $F_m^{(n)}$ to be a $\mathbb{P}^{n-1}$-fibration (encoded by $\nu_1, \cdots, \nu_n$) over the base-$\mathbb{P}^1$ (encoded by ν_{n+1}, ν_{n+2}).

The mutually defining relation,

$$\text{(2.14)} \qquad \sum_{i=1}^{n+2} Q_i^a \nu_i^\kappa = 0, \qquad \begin{cases} a = 1, 2; \\ \kappa = 1, \cdots, n. \end{cases}$$

specifies the integral components ν_i^κ only up to linear combinations $\nu_i^\kappa \simeq \sum_\lambda c^\kappa{}_\lambda \nu_i^\lambda$, so the integral n-vectors $\vec{\nu}_i$ are defined only up to overall $\mathrm{GL}(n; \mathbb{Z})$ transformations. Analogously, the GLSM gauge charges Q_i^a are defined only up to linear combinations $Q_i^a \simeq \sum_b C^a{}_b Q_i^b$, so the secondary fan generators $\vec{Q}_i$ are defined only up to $\mathrm{GL}(2; \mathbb{Z})$ transformations. Verifying certain additional conditions [29], the Q^a-vectors are identified as the Mori vectors for the toric variety specified in (2.13).

The toric specification (2.13) is detailed [13–15, 30, 31]: Each top-dimensional cone $\sigma_I \in \Sigma_{F_m^{(n)}}$ (over a facet of $\Delta^\star_{F_m^{(n)}}$) encodes a $\mathbb{C}^n$-like chart of $F_m^{(n)}$, glued together as per their intersection, $\sigma_I \cap \sigma_J \subset \Sigma_{F_m^{(n)}}$. The complete hierarchy of these mutual intersections, down to the 1-cones ν_i, fully specifies not only the space $F_m^{(n)}$ but also its toric holomorphic submanifolds and *their* mutual intersections [31]. In particular, each of these 1-cones specifies a divisor defined as the zero locus of a (Cox) variable, such as the $\nu_i \mapsto X_i$ in (2.13), which in turn generate the homogeneous coordinate ring of the toric space [32].

2.4. The anticanonical system

Another key holomorphic characteristic of the ambient space in which we seek Calabi-Yau hypersurfaces,

$$\text{(2.15)} \qquad \left(X_m^{(n-1)} \subset \left(F_m^{(n)} := \{ p_0(x,y) = 0 \} \right) \right) \in \begin{bmatrix} \mathbb{P}^n \\ \mathbb{P}^1 \end{bmatrix} \begin{array}{|c|c} 1 & n \\ m & 2-m \end{array} ,$$

$$p_0(x,y) = x_0 y_0^m + x_1 y_1^m,$$

are the anticanonical sections $\Gamma \left(\mathcal{K}^*_{F_m^{(n)}} = \mathcal{O}(2^{\;n}_{-m}) \big|_{F_m^{(n)}} \right)$, i.e., degree-$(2^{\;n}_{-m})$ defining equations $q(x,y) = 0$. For $m = 0$ and 1, all $3\binom{2n-1}{n}$ such sections are regular (x,y)-polynomials on $A = \mathbb{P}^n \times \mathbb{P}^1$, while for $m = 2$ only $2\binom{2n-1}{n} = \binom{2n}{n}$ are regular, global polynomials. The remaining $\binom{2n-1}{n}$ sections are *non-polynomial* [19, 33], and stem from certain 1-forms on $A = \mathbb{P}^n \times \mathbb{P}^1$. In the general, $m \geqslant 3$ cases, those 1-forms are the sole source

of $\mathcal{K}^*_{F^{(n)}}$-sections, as evident from the Koszul resolution of the restriction $\mathcal{O}_A(\genfrac{}{}{0pt}{}{\tilde{m}}{2-m}) \to \mathcal{O}(\genfrac{}{}{0pt}{}{n}{2-m})|_{F^{(n)}_m}$ [1, 2].

For the required total degree $(\genfrac{}{}{0pt}{}{n}{2-m})$ and $m \geqslant 3$, we list products of non-negative powers of the variables (2.12) except p_0, all of which must have at least one $\mathfrak{s}(x, y)$-factor:

(2.16)

$$q(x, y; \lambda) := \sum_{k=0}^{n-1} \sum_{\ell=0}^{km+2} \underbrace{c_\ell^{(n-k-1)}(x_2, \cdots, x_n)}_{\deg = \binom{n-k-1}{0}} \underbrace{\left(y_0^{km+2-\ell} y_1^\ell\right)}_{+\binom{0}{2+km}} \underbrace{\mathfrak{s}(x, y; \lambda)^{k+1}}_{+ (k+1)\binom{1}{-m}}.$$

where the $c_\ell^{(n-k-1)}$ are regular polynomials of their arguments, and the mod-p_0 equivalence is inherited from the $\mathfrak{s}$-factor. This may be seen as a generalization of Construction 1 and (2.10).

The toric rendition encodes the anticanonical sections by the *polar* [13–15] of the spanning polytope, $\Delta^\star_{F^{(n)}_m} \gg \Sigma_{F^{(n)}_m}$ (such as in (2.13), left and middle):

(2.17) $$(\Delta^\star_{F^{(n)}_m})^\circ \overset{\text{def}}{=} \{\, u\colon \ \langle v, u\rangle + 1 \geqslant 0, \quad v \in \Delta^\star_{F^{(n)}_m} \,\}.$$

These *regular* anticanonical sections are then all of the form [10]:

(2.18) $$H^0(F^{(n)}_m, \mathcal{K}^*) \ni \sum_{\mu \in M \cap (\Delta^\star_{F^{(n)}_m})^\circ} a_\mu \left(\prod_{\nu_i \lessdot \Delta^\star_{F^{(n)}_m}} X_i^{\langle \nu_i, \mu\rangle + 1} \right)$$

where $\nu_i \lessdot \Delta^\star_X$ are the vertices of $\Delta^\star_X$, i.e., the 1-cone generators of Σ_X, with N-lattice co-prime coordinates specifying the Cox variables X_i, and M is the lattice dual to N. This yields

(2.19) $$\begin{aligned} H^0(F^{(2)}_m, \mathcal{K}^*) \ni\ & X_1 X_2 \big(c_0^1 X_3^2 + c_1^1 X_3 X_4 + c_2^1 X_4^2 \big) \\ & + X_1^2 \big(c_0^0 X_3^{m+2} + c_1^0 X_3^{m+1} X_4 + \cdots + c_{m+1}^0 X_3 X_4^{m+1} + c_{m+2}^0 X_4^{m+2} \big), \end{aligned}$$

exactly matching the $n=2$ case of (2.16) after renaming the variables as in (2.12b) and having simplified, e.g., $c_0^1(X_2) = c_0^1 X_2$ and $c_0^0(X_2) = c_0^0$, so the coefficients c_i^{n-k-1} in (2.19) are plain constants. These regular polynomials indeed all have an overall factor of $X_1 \leftrightarrow \mathfrak{s}(x, y)$, and so fully agree with (2.16).

The "tuning" of $q(x, y; \lambda)$ in (2.16) to (2.1) builds the moduli space of generalized complete intersections such as (2.15) over the deformation space (even if discrete) of the general type ambient spaces such as (2.1). While we defer a detailed study of this hierarchy, let us consider a few examples.

2.5. Discrete deformations

Consider the Hirzebruch scroll $F_{5;0}^{(3)} = \{x_0\, y_0^5 + x_1\, y_1^5\} \in \left[\begin{smallmatrix} \mathbb{P}^3 \\ \mathbb{P}^1 \end{smallmatrix}\middle\|\begin{smallmatrix} 1 \\ 5 \end{smallmatrix}\right]$, with its

	X_1	X_2	X_3	X_4	X_5
$\Sigma_{F_5}^{(3)}$	-1	1	0	0	-5
	-1	0	1	0	-5
	0	0	0	1	-1
Q^1	1	1	1	0	0
Q^2	-5	0	0	1	1
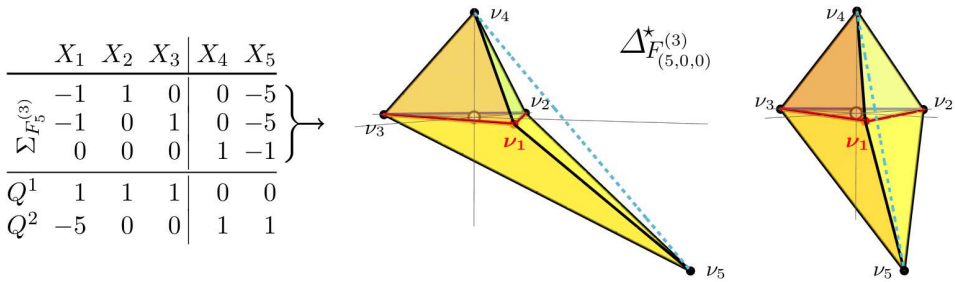
Figure 1: The toric specification of $F_5^{(3)}$ (left) and its spanning polytope (middle and right)

unique degree-$\left(\begin{smallmatrix} -1 \\ -5 \end{smallmatrix}\right)$ directrix, $\mathfrak{s}(x,y)$; see (2.11). The reparametrization (2.12a) leads to the toric rendition in Figure 1, its spanning polytope, $\Delta_{F_{(5,0,0)}^{(3)}}^\star$, depicted to the right of the tabulation from two vantage points for clarity. It is non-convex at the saddle-point, ν_1. The horizontal polygon spans the fan of the fibre-$\mathbb{P}^2$ and $-\sum_{i=1}^3 Q^2(X_i) = 5$ is the total twist in this $\mathbb{P}^2$-bundle over $\mathbb{P}^1$.

A simple deformation. Consider deforming the $n=3$, $m=5$ central case (2.1) in the $\left[\begin{smallmatrix} \mathbb{P}^3 \\ \mathbb{P}^1 \end{smallmatrix}\middle\|\begin{smallmatrix} 1 \\ 5 \end{smallmatrix}\right]$ deformation family, which corresponds to the toric specification of $F_5^{(3)}$ in Figure 1:

$$(2.20a) \qquad p_1(x,y) = x_0\, y_0^5 + x_1\, y_1^5 + x_2\, y_1^4 y_0^1.$$

It admits two algebraically independent directrices:

$$(2.20b) \qquad \left(\begin{smallmatrix} -1 \\ -4 \end{smallmatrix}\right): \quad \mathfrak{s}_{1,1}(x,y) = \frac{x_0\, y_0}{y_1^5} + \frac{x_2}{y_1^4} - \frac{x_1}{y_0^4} \pmod{p_1},$$
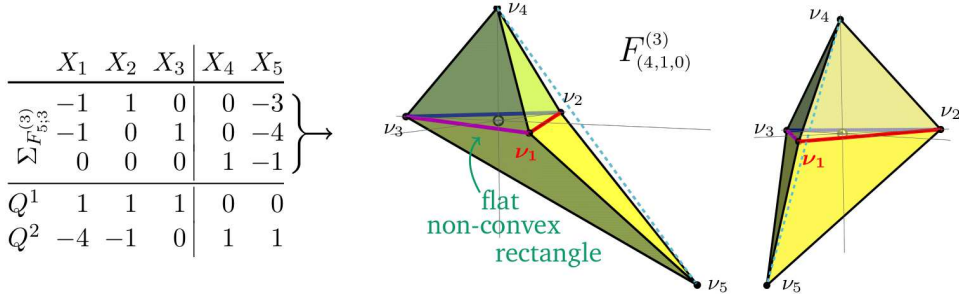
$$(2.20c) \qquad \left(\begin{smallmatrix} -1 \\ -1 \end{smallmatrix}\right): \quad \mathfrak{s}_{1,2}(x,y) = \frac{x_0}{y_1} - \frac{x_2}{y_0} - \frac{x_1\, y_1^4}{y_0^5} \pmod{p_1}.$$

As above, the reparametrization

$$(2.21) \qquad \begin{aligned} &(x_0, x_1, x_2, \cdots; y_0, y_1) \to (p_1, \mathfrak{s}_{1,1}, \mathfrak{s}_{1,2}, \cdots; y_0, y_1), \\ &\det\left[\frac{\partial(p_1, \mathfrak{s}_{1,1}, \mathfrak{s}_{1,2}, \cdots; y_0, y_1)}{\partial(x_0, x_1, x_2, \cdots; y_0, y_1)}\right] = 4 \end{aligned}$$

again has a constant Jacobian, and produces the toric rendition:
(2.22)

where the Cox variables are $X_1 = \mathfrak{s}_{1,1}$, $X_2 = \mathfrak{s}_{1,2}$, $X_3 = x_3$, $X_4 = y_0$ and $X_5 = y_1$.

Another simple deformation. Another simple deformation within the $\left[\begin{smallmatrix}\mathbb{P}^3\\\mathbb{P}^1\end{smallmatrix}\middle\|\begin{smallmatrix}1\\5\end{smallmatrix}\right]$ deformation family,

$$(2.23a) \qquad \left(\tfrac{1}{5}\right): \quad p_2(x,y) = x_0\, y_0^5 + x_1\, y_1^5 + x_2\, y_1^3\, y_0^2$$

admits two algebraically independent directrices:

$$(2.23b) \qquad \left(\begin{smallmatrix}-1\\-3\end{smallmatrix}\right): \quad \mathfrak{s}_{2,1}(x,y) = \frac{x_0\, y_0^2}{y_1^5} + \frac{x_2}{y_1^3} - \frac{x_1}{y_0^3} \pmod{p_2},$$

$$(2.23c) \qquad \left(\begin{smallmatrix}-1\\-2\end{smallmatrix}\right): \quad \mathfrak{s}_{2,2}(x,y) = \frac{x_0}{y_1^2} - \frac{x_2}{y_0^2} - \frac{x_1 y_1^3}{y_0^5} \pmod{p_2}.$$

As above, the reparametrization

$$(2.24) \qquad \begin{aligned} &(x_0, x_1, x_2, \cdots; y_0, y_1) \to (p_2, \mathfrak{s}_{2,1}, \mathfrak{s}_{2,2}, \cdots; y_0, y_1), \\ &\det\left[\frac{\partial(p_2, \mathfrak{s}_{2,1}, \mathfrak{s}_{2,2}, \cdots; y_0, y_1)}{\partial(x_0, x_1, x_2, \cdots; y_0, y_1)}\right] = 4 \end{aligned}$$

again has a constant Jacobian and produces the toric rendition:
(2.25)
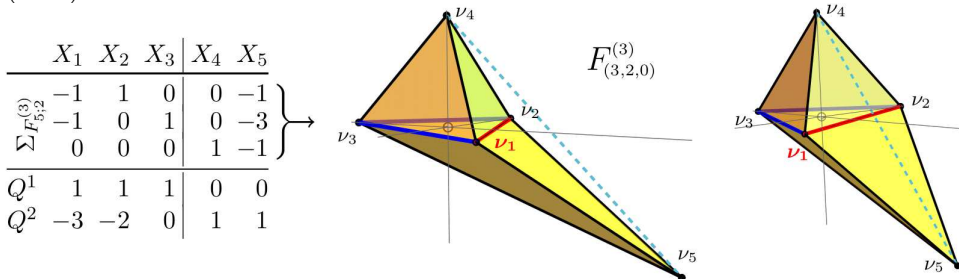
where the Cox variables are $X_1 = \mathfrak{s}_{2,1}$, $X_2 = \mathfrak{s}_{2,2}$, $X_3 = x_3$, $X_4 = y_0$ and $X_5 = y_1$.

A double deformation. Consider a further, $\mathbb{P}^1$-symmetrizing deformation of (2.23a):

$$(2.26a) \quad \deg = (\tfrac{1}{5}): \qquad p_3(x, y) = x_0\, y_0^5 + x_1\, y_1^5 + x_2\, y_1^3\, y_0^2 + x_3\, y_1^2\, y_0^3$$

and admits three algebraically independent directrices:

$$(2.26b) \quad \deg = (\tfrac{-1}{-2}): \quad \mathfrak{s}_{3,1}(x, y) = \frac{x_0}{y_1^2} - \frac{x_2}{y_0^2} - \frac{x_3\, y_1}{y_0^3} - \frac{x_1\, y_1^3}{y_0^5} \pmod{p_3},$$

$$(2.26c) \quad \deg = (\tfrac{-1}{-2}): \quad \mathfrak{s}_{3,2}(x, y) = \frac{x_0\, y_0^3}{y_1^5} + \frac{x_2\, y_0}{y_1^3} + \frac{x_3}{y_1^2} - \frac{x_1}{y_0^2} \pmod{p_3},$$

$$(2.26d) \quad \deg = (\tfrac{-1}{-1}): \quad \mathfrak{s}_{3,3}(x, y) = \frac{x_0\, y_0^2}{y_1^3} + \frac{x_2}{y_1} - \frac{x_3}{y_0} - \frac{x_1\, y_1^2}{y_0^3} \pmod{p_3}.$$

These $\mathfrak{s}_{3,i}(x, y)$ have four monomials instead of just two in (2.12a). As before, the reparametrization

$$(2.27) \qquad (x_0, x_1, x_2, x_3, \cdots; y_0, y_1) \rightarrow (p_3, \mathfrak{s}_{3,1}, \mathfrak{s}_{3,2}, \mathfrak{s}_{3,3}, \cdots; y_0, y_1),$$

has a constant Jacobian, $\det\left[\frac{\partial(p_3, \mathfrak{s}_{3,1}, \mathfrak{s}_{3,2}, \mathfrak{s}_{3,3}, \cdots; y_0, y_1)}{\partial(x_0, x_1, x_2, x_3, \cdots; y_0, y_1)}\right] = 8$. The 3-dimensional hypersurface $p_3(x, y) = 0$ has the straightforward toric rendition with the Cox variables $X_i = \mathfrak{s}_{3,i}(x, y)$, $X_4 = y_0$ and $X_5 = y_1$:
(2.28)

	X_1	X_2	X_3	X_4	X_5
$\Sigma_{F_{5;\epsilon_3}^{(3)}}$	-1	1	0	0	0
	-1	0	1	0	-1
	0	0	0	1	-1
Q^1	1	1	1	0	0
$\widetilde{Q}^2$	-2	-2	-1	1	1

$\approx_{\mathbb{R}}$

	X_1	X_2	X_3	X_4	X_5
$\Sigma_{F_{5;\epsilon_3}^{(3)}}$	-1	1	0	0	0
	-1	0	1	0	-1
	0	0	0	1	-1
Q^1	1	1	1	0	0
Q^2	-1	-1	0	1	1

where the choice of Q-charges on the far left (bottom two rows) follows from the change of variables (2.27) with (2.26), which simplifies to $Q^2 = \widetilde{Q}^2 + Q^1$, reflecting the $F_5^{(3)} \approx_{\mathbb{R}} F_2^{(3)}$ diffeomorphism of Hirzebruch scrolls. In turn, the $\Sigma_{F_{5;\epsilon_3}^{(3)}} < \Delta^\star_{F_{(1,1,0)}^{(3)}}$ specification (2.28) unambiguously specifies this latter choice of 5-vectors, (Q^1, Q^2), as the correct Mori vectors [29], consistent with a star-triangulation of the spanning polytope and the corresponding

simplicial unit subdivision of the fan. This type of discrete deformations $F_m^{(n)} \rightsquigarrow F_{m \,(\mathrm{mod}\, n)}^{(n)}$ have been seen to affect string compactifications since early on, notably in the simplest form, $F_2^{(2)} \rightsquigarrow F_0^{(2)}$ [23, 24]. By effectively reducing the negativity of X_1, X_2 and the total twist from 5 to 2, the resulting toric specification $F_{(1,1,0)}^{(3)}$ in (2.28) no longer features directrices as negative as (2.26b)–(2.26c), and deforms the non-Fano hypersurface (2.26d) into the almost Fano $F_{(1,1,0)}^{(3)}$.

A comparison. Two rather distinct-looking members of this deformation family of 3-folds, the $y_0 \leftrightarrow y_1$-symmetrized versions of (2.20a), and an asymmetric deformation of (2.23a):
(2.29)

		X_1	X_2	X_3	X_4	X_5
		-1	1	0	0	-2
$\Sigma_{F_{(2,0,0)}^{(3)}}$		-1	0	1	0	-2
		0	0	0	1	-1
Q^1		1	1	1	0	0
Q^2		-2	0	0	1	1

$$\begin{bmatrix} \mathbb{P}^3 \,\big\|\, 1 \\ \mathbb{P}^1 \,\big\|\, 5 \end{bmatrix} \ni \begin{array}{l} x_0\,y_0^5 + x_1\,y_1^5 + x_2\,y_0^4\,y_1 + x_3\,y_0\,y_1^4 = 0 \\ x_0\,y_0^5 + x_1\,y_1^5 + x_2\,y_0^4\,y_1 + x_3\,y_0^3\,y_1^2 = 0 \end{array} \;\Rightarrow\;$$

$$\Rightarrow \begin{cases} \widetilde{Q}^1(x_0,\cdots,y_1) = (1,1,1,0,0) \\ \widetilde{Q}^2(x_0,\cdots,y_1) = (-3,-1,-1,1,1) \end{cases}$$

Each of them admits a (different) collection of one degree-$\left(\begin{smallmatrix}1\\-3\end{smallmatrix}\right)$ and *two* independent degree-$\left(\begin{smallmatrix}1\\-1\end{smallmatrix}\right)$ directrices. Via analogous constant-Jacobian changes of variables, they both lead to the same toric $F_{(3,1,1)}^{(3)} \approx_{\mathbb{R}} F_{(2,0,0)}^{(3)}$, where the last equivalence is again the toric rendition of Wall's diffeomorphism [20]. This shows that there exist rather nontrivial identifications within the coarse parameter space of $\left[\begin{smallmatrix}\mathbb{P}^3\,\|\,1\\\mathbb{P}^1\,\|\,5\end{smallmatrix}\right]$. For each $n \geqslant 2$, $F_{(2,0,\cdots)}^{(n)}$ is almost Fano: both its spanning and its Newton polytope is convex and reflexive, although $\Delta^\star_{F_{(2,0\cdots)}^{(n)}}$ has a degree-2 edge, which is polar to a *double* $(n-2)$-face in $\Delta_{F_{(2,0\cdots)}^{(n)}}$.

By modifying the spanning polytope and its central fan, $\Delta^\star_{F_{\vec{m}}^{(n)}} \gg \Sigma_{F_{\vec{m}}^{(n)}}$, these and other deformations also modify the Newton polytope, both its regular part and the extension, and thereby also the entire anticanonical system.

The general picture. The hypersurfaces (2.20a), (2.23a) and (2.26a) are evidently deformations of the $n=3$, $m=5$ case of (2.1). Consequently, $F_{(4,1,0)}^{(3)}$, $F_{(3,2,0)}^{(3)}$ and $F_{(2,2,1)}^{(3)} \approx_{\mathbb{R}} F_{(1,1,0)}^{(3)}$ are all explicit (discrete) deformations of $F_5^{(3)}$. The evident generalizations of these explicit constructions suggest:

Claim 1. *For any integral n-tuple $\vec{m}$ with $\sum_{i=1}^n m_i = m$, the $\vec{m}$-twisted $\mathbb{P}^{n-1}$-bundle over $\mathbb{P}^1$ may be identified with toric variety $F_{\vec{m}}^{(n)}$, specified by the two Mori $(n+2)$-vectors, $Q^1 = (1,\cdots,1;0,0)$ and $Q^2 = (-\vec{m};1,1)$. They are all (discrete) deformations of $F_m^{(n)}$, specified by $Q^2 = (-m,0,\cdots,0;1,1)$,*

and may all be located in specific regions of $\left[\begin{smallmatrix}\mathbb{P}^n \\ \mathbb{P}^1\end{smallmatrix}\middle\|\begin{smallmatrix}1 \\ m\end{smallmatrix}\right]$, the full deformation family of simple degree-$\binom{1}{m}$ hypersurfaces in $\mathbb{P}^n \times \mathbb{P}^1$. Equivalently, $F^{(n)}_{\vec{m}} \approx \mathbb{P}\big(\mathcal{O}_{\mathbb{P}^1} \oplus \bigoplus_i \mathcal{O}_{\mathbb{P}^1}(m_i)\big)$.

Recall that $h^1(F^{(n)}_m, T) < h^0(F^{(n)}_m, T)$ implies that all $F^{(n)}_m$ are effectively rigid, so that their space of complex structures is discrete, which suggests the general situation illustrated in Figure 2. The concrete examples (2.20a), (2.23a),
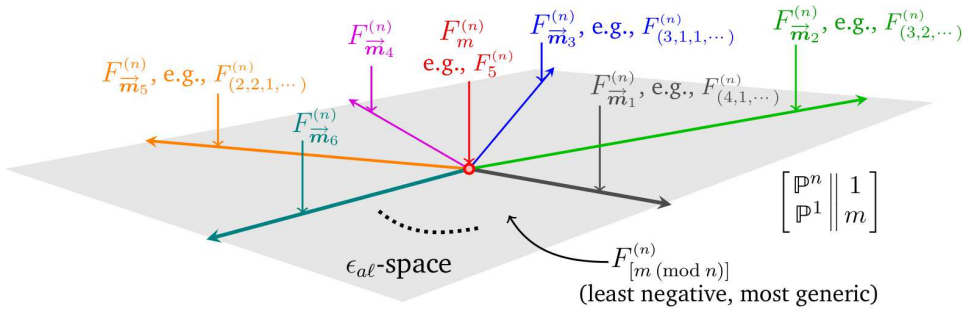
Figure 2: A rough sketch of the full deformation family of degree-$\binom{1}{m}$ hypersurfaces in $\mathbb{P}^n \times \mathbb{P}^1$

(2.26a) and (2.29) do not have any explicit coefficients shown since those are easily absorbed by (x, y)-rescaling. However, writing them out explicitly shows that for each parameter, only $\epsilon_{a\ell} \neq 0$ vs. $\epsilon_{a\ell} = 0$ is distinguished: all these models are infinitesimally near each other. For a related but differently constructed explicit deformation family containing $F^{(2)}_2$ and $F^{(2)}_0$ see [19, 22]. Either way, the result of (2.29) shows that the coarse $\epsilon_{a\ell}$-parameter space in (2.2) is subject to highly nontrivial identifications.

3. Calabi-Yau subspaces

We now turn to Calabi-Yau hypersurfaces in the *central* hypersurface in the deformation family $\left[\begin{smallmatrix}\mathbb{P}^n \\ \mathbb{P}^1\end{smallmatrix}\middle\|\begin{smallmatrix}1 \\ m\end{smallmatrix}\right]$; see Figure 2. Less special cases then include deformations such as discussed in the previous section, and the deformation space of Calabi-Yau hypersurfaces therein builds atop the effectively discrete one in Figure 2.

3.1. Tyurin degeneration: Calabi-Yau matryoshke

The explicit expansions $(2.16) \approx (2.19)$ show that for $m \geqslant 3$, every anticanonical section of $F_m^{(n)}$ factorizes:

$$(3.1) \qquad \begin{aligned} H^0(F_m^{(n)}, \mathcal{K}^*) \ni q(x, y) &= \mathfrak{c}(x, y) \cdot \mathfrak{s}(x, y), \\ \deg(\mathfrak{s}) = \left(\begin{smallmatrix} 1 \\ -m \end{smallmatrix} \right), \quad & \deg(\mathfrak{c}) = \left(\begin{smallmatrix} n-1 \\ 2 \end{smallmatrix} \right), \end{aligned}$$

$$(3.2) \qquad \mathfrak{c}(x, y) := \sum_{k=0}^{n-1} \sum_{\ell=0}^{km+2} c_\ell^{(n-k-1)}(x_2, \cdots, x_n) \left(y_0^{km+2-\ell} y_1^\ell \right) \mathfrak{s}^k(x, y).$$

Thus, all anticanonical (Calabi-Yau) hypersurfaces *reduce* to a union of two components:

$$(3.3) \qquad m \geqslant 3, \quad F_m^{(n)} \supset \left(X_m^{(n-1)} := q^{-1}(0) \right) = \left(C_m := \mathfrak{c}^{-1}(0) \right) \cup \left(S_m := \mathfrak{s}^{-1}(0) \right).$$

As divisors in $F_m^{(n)}$, $[X_m^{(n-1)}] = [C_m] + [S_m]$. With generic coefficient polynomials $c_i^{(n-k-1)}(x_2, \cdots, x_n)$, the component $\mathfrak{c}^{-1}(0) \subset F_m^{(n)}$ is non-singular and holomorphic, and so irreducible. With $\mathfrak{s}^{-1}(0)$ having been named the *directrix* [16], we call $\mathfrak{c}^{-1}(0)$ the *complementrix*.

Singularity. Being *reducible* for $m \geqslant 3$, the generic Calabi-Yau $(n-1)$-fold $X_m^{(n-1)} \subset F_m^{(n)}$ is singular precisely at the intersection of its components:

$$(3.4) \qquad \operatorname{Sing} X_m^{(n-1)} = C_m \cap S_m \in \left[\begin{matrix} \mathbb{P}^n \\ \mathbb{P}^1 \end{matrix} \middle\| \begin{matrix} 1 \\ m \end{matrix} \middle| \begin{matrix} 1 & n-1 \\ -m & 2 \end{matrix} \right].$$

The row-wise sum of degrees shows that $\operatorname{Sing} X_m^{(n-1)}$ is itself a Calabi-Yau subspace, now of codimension-2 in $F_m^{(n)}$ — a Calabi-Yau *matryoshka*[2], a Calabi-Yau-within-Calabi-Yau. The reducible Calabi-Yau hypersurface (3.3) and its codimension-1 singular set are sketched in Figure 3; it fits within the framework of "Constructive Calabi-Yau manifolds" [34] and exhibits the so-called Tyurin degeneration [35].

---

[2]We have recently learned that C. Doran has been independently using the same term and metaphor for such iteratively nested chains of Calabi-Yau subspaces in presentations.
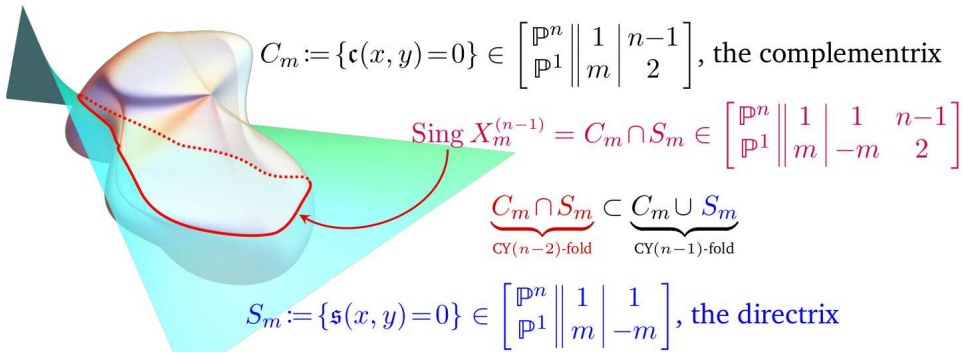
$$C_m := \{\mathfrak{c}(x,y) = 0\} \in \begin{bmatrix} \mathbb{P}^n \\ \mathbb{P}^1 \end{bmatrix} \begin{vmatrix} 1 \\ m \end{vmatrix} \begin{matrix} n-1 \\ 2 \end{matrix} \end{bmatrix}, \text{ the complementrix}$$

$$\text{Sing } X_m^{(n-1)} = C_m \cap S_m \in \begin{bmatrix} \mathbb{P}^n \\ \mathbb{P}^1 \end{bmatrix} \begin{vmatrix} 1 \\ m \end{vmatrix} \begin{matrix} 1 \\ -m \end{matrix} \begin{matrix} n-1 \\ 2 \end{matrix} \end{bmatrix}$$

$$\underbrace{C_m \cap S_m}_{\text{CY}(n-2)\text{-fold}} \subset \underbrace{C_m \cup S_m}_{\text{CY}(n-1)\text{-fold}}$$

$$S_m := \{\mathfrak{s}(x,y) = 0\} \in \begin{bmatrix} \mathbb{P}^n \\ \mathbb{P}^1 \end{bmatrix} \begin{vmatrix} 1 \\ m \end{vmatrix} \begin{matrix} 1 \\ -m \end{matrix} \end{bmatrix}, \text{ the directrix}$$

Figure 3: The generic Calabi-Yau hypersurface $X_m^{(n-1)} \subset F_m^{(n)}$ for $m \geqslant 3$ and its codimension-1 singularity

Owing to the simple forms of $p_0(x,y)$ and $\mathfrak{s}(x,y)$ and the reparametrization (2.12), it follows that
(3.5)
$$(x_0 y_0{}^m + x_1 y_1{}^m) =: p_0(x,y) = 0 = \mathfrak{s}(x,y) := \left(\frac{x_0}{y_1{}^m} - \frac{x_1}{y_0{}^n}\right) \quad \Leftrightarrow \quad x_0 = 0 = x_1,$$

which is not surprising, given the constant-Jacobian reparametrization equivalence $(p_0, \mathfrak{s}, \dots) \approx (x_0, x_1, \dots)$ found in (2.12a). This in turn leaves

$$(3.6) \quad {}^\sharp X_m^{(n-2)} = \text{Sing } X_m^{(n-1)}$$
$$= \left\{ \sum_{\ell=0}^{2} c_\ell^{(n-1)}(x_2, \cdots, x_n)(y_0{}^{2-\ell} y_1{}^\ell) = 0 \right\} \in \begin{bmatrix} \mathbb{P}^{n-2} \\ \mathbb{P}^1 \end{bmatrix} \begin{vmatrix} n-1 \\ 2 \end{vmatrix} \end{bmatrix},$$

which is nonsingular for generic choices of the coefficient functions $c_\ell^{(n-1)}(x_2, \cdots, x_n)$ — and is a regular anticanonical (Calabi-Yau) hypersurface.

Order matters. The left-to-right ordering of the hypersurfaces in $\begin{bmatrix} \mathbb{P}^n \\ \mathbb{P}^1 \end{bmatrix} \begin{vmatrix} 1 \\ m \end{vmatrix} \begin{matrix} 1 \\ -m \end{matrix} \begin{matrix} n-1 \\ 2 \end{matrix} \end{bmatrix}$ (3.4) *is relevant* within the framework of *generalized complete intersections* [1, 2, 4] and the |-separation signifies this: The 2nd, degree-$\binom{1}{-m}$ degree hypersurface $\mathfrak{s}^{-1}(0)$ is well defined only within the 1st, degree-$\binom{1}{m}$ hypersurface $F_m^{(n)} := p_0^{-1}(0)$. Away from $p_0^{-1}(0)$, the *equivalence class* (2.11) is holomorphic, but its zero-locus $\mathfrak{s}^{-1}(0)$ is not well defined. In the toric rendition (2.13), $p_0(x,y) = 0$ and this "tuning" hold by the definition of $F_m^{(n)}$; see (2.12b). In contrast, the 3rd, degree-$\binom{n-1}{2}$ defining polynomial (3.2) of the complementrix is regular on all of $A = \mathbb{P}^n \times \mathbb{P}^1$, and

the zero-locus $\mathfrak{c}^{-1}(0)$ is well defined everywhere on A, including $p_0^{-1}(0)$ and $\mathfrak{s}^{-1}(0)$.

Owing to (3.5) and the reduction (3.4)$\rightsquigarrow$(3.6), the common zero-locus $p_0^{-1}(0) \cap \mathfrak{s}^{-1}(0)$ is equivalent to the $x_0 = 0 = x_1$ subspace, $\mathbb{P}^{n-2} \times \mathbb{P}^1 \subset A$. Indeed, for the $n = 2$ case, the original Hirzebruch *surface,* the directrix is equivalent to $\mathbb{P}^0 \times \mathbb{P}^1$ — the simple (algebraic) line of self-intersection $-m$ within $F_m^{(2)}$ [12, 16]. Therein, the complementrix is the anticanonical hypersurface, which is indeed two points — the Calabi-Yau 0-fold:

$$(3.7) \qquad \begin{bmatrix} \mathbb{P}^2 \\ \mathbb{P}^1 \end{bmatrix} \left\| \begin{matrix} 1 \\ m \end{matrix} \right| \left. \begin{matrix} 1 \\ -m \end{matrix} \right| \left. \begin{matrix} 1 \\ 2 \end{matrix} \right. \overset{(3.5)}{\approx} \begin{bmatrix} \mathbb{P}^0 \\ \mathbb{P}^1 \end{bmatrix} \left\| \begin{matrix} 1 \\ 2 \end{matrix} \right. : \quad \mathfrak{c}(x, y) = x_2 \, y_0 \, y_1 \quad \text{where } x_2 \simeq \lambda x_2 \neq 0,$$

which is the singularity, $\operatorname{Sing} X_m^{(1)}$. Thus, $X_m^{(1)} \in \begin{bmatrix} \mathbb{P}^2 \\ \mathbb{P}^1 \end{bmatrix}\left\|\begin{matrix}1\\m\end{matrix}\right|\left.\begin{matrix}2\\2-m\end{matrix}\right.$ is a twice-pinched torus; see Figure 4.
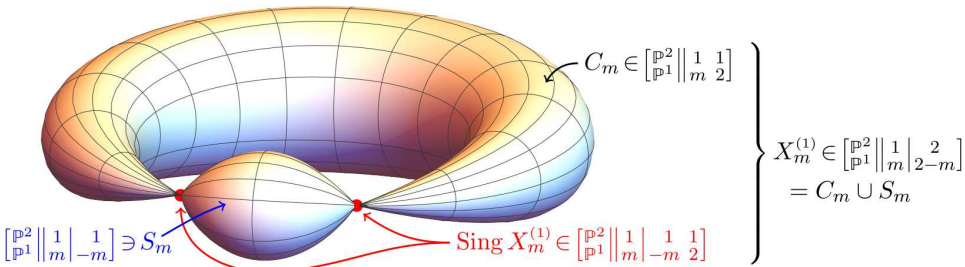
Figure 4: The general, $m \geqslant 3$, case of the Calabi-Yau subspaces in a Hirzebruch surface, $F_m^{(2)}$

Being exceptional. The foregoing constructions explicitly depend on the central choice (2.1) within the deformation family $\begin{bmatrix} \mathbb{P}^n \\ \mathbb{P}^1 \end{bmatrix}\left\|\begin{matrix}1\\m\end{matrix}\right.$, and cannot be completed for the deformed choices (2.2). In particular, the total degree-$\left(\begin{smallmatrix}1\\-m\end{smallmatrix}\right)$ multiple of $p_{\vec{\epsilon}}(x, y)$ is

$$(3.8) \qquad \frac{p_{\vec{\epsilon}}(x, y)}{(y_0 \, y_1)^m} = \left(\frac{x_0}{y_1^m} + \frac{x_1}{y_0^m} \right) + \sum_{a=0}^{n} \sum_{\ell=1}^{m-1} \epsilon_{a\ell} \, x_a \, y_0^{-\ell} y_1^{\ell-m}.$$

The $\epsilon_{a\ell}$-expansion contains rational monomials with mixed denominators and a y_0, y_1-independent numerator when $\epsilon_{a\ell} \neq 0$, each of which has a pole

in both coordinate charts in $\mathbb{P}^1$ and so cannot be holomorphic in the manner of (2.11)[3].

This proves the central hypersurface (2.1) to be the unique one in the deformation family $\left[\begin{smallmatrix}\mathbb{P}^n\\\mathbb{P}^1\end{smallmatrix}\middle\|\begin{smallmatrix}1\\m\end{smallmatrix}\right]$ that has an irreducible directrix with the maximally negative self-intersection, $[S_m]^n = -(n-1)m$. Consequently, the anticanonical hypersurfaces $X_m^{(n-1)} \subset F_m^{(n)}$ are necessarily singular only for this central case. The smooth Calabi-Yau 3-folds of the form (2.15) reported in [1] refer[4] to non-central cases (2.2), some of which were discussed in §2.5.

The above facts add to the connectivity among (generalized) complete intersection Calabi-Yau n-folds. Suffice it here to provide an example, deferring a more detailed analysis to a separate effort:

1) The *generic* Calabi-Yau 3-folds in the deformation family $\left[\begin{smallmatrix}\mathbb{P}^4\\\mathbb{P}^1\end{smallmatrix}\middle\|\begin{smallmatrix}1\\5\end{smallmatrix}\middle|\begin{smallmatrix}4\\-3\end{smallmatrix}\right]$ are smooth and are diffeomorphic to generic members in $\left[\begin{smallmatrix}\mathbb{P}^4\\\mathbb{P}^1\end{smallmatrix}\middle\|\begin{smallmatrix}1\\1\end{smallmatrix}\middle|\begin{smallmatrix}4\\1\end{smallmatrix}\right]$ of *regular* complete intersections. This then connects at least some gCICYs into the "web of Calabi-Yau 3-folds" [36–39].

2) The *special* Calabi-Yau 3-folds in the deformation family $\left[\begin{smallmatrix}\mathbb{P}^4\\\mathbb{P}^1\end{smallmatrix}\middle\|\begin{smallmatrix}1\\5\end{smallmatrix}\middle|\begin{smallmatrix}4\\-3\end{smallmatrix}\right]$ using the *central,* Hirzebruch-like defining equation (2.1) are all singular (Tyurin-degenerate, see below), but their singular set is itself a smooth Calabi-Yau (K3) 2-fold, thus connecting to the web of Calabi-Yau 2-folds.

Tyurin degeneration. By reducing for $m \geqslant 3$ to a union $X_m^{(n-1)} = (C_m \cup S_m)$ (3.3) where $\mathfrak{X} := (C_m \cap S_m)$ is a codimension-2 Calabi-Yau space (3.4), each Calabi-Yau $X_m^{(n-1)}$ hypersurface in the *central* Hirzebruch scroll (2.1), $\left(F_m^{(n)} := p_0^{-1}(0)\right)$, is *Tyurin degenerate* [35]. In the bi-projective embedding and restricting to $\mathfrak{X} := {}^\sharp X_m^{(n-2)} \in \left[\begin{smallmatrix}\mathbb{P}^n\\\mathbb{P}^1\end{smallmatrix}\middle\|\begin{smallmatrix}1\\m\end{smallmatrix}\middle|\begin{smallmatrix}1\\-m\end{smallmatrix}\middle|\begin{smallmatrix}n-1\\2\end{smallmatrix}\right]$, the adjunction relations

$$(3.9) \quad T_{\mathfrak{X}} \hookrightarrow T_{C_m}\big|_{\mathfrak{X}} \twoheadrightarrow \mathcal{O}_A\binom{n-1}{2}\big|_{\mathfrak{X}}, \quad \text{and} \quad T_{\mathfrak{X}} \hookrightarrow T_{S_m}\big|_{\mathfrak{X}} \twoheadrightarrow \mathcal{O}_A\binom{1}{-m}\big|_{\mathfrak{X}}$$

identify the two rightmost sheaves as the normal sheaves of $\mathfrak{X} \subset C_m$ and $\mathfrak{X} \subset S_m$, respectively. Then,

$$(3.10) \quad \mathcal{O}_A\binom{n-1}{2}\big|_{\mathfrak{X}} \otimes \mathcal{O}_A\binom{1}{-m}\big|_{\mathfrak{X}} = \mathcal{O}_A\binom{n}{2-m}\big|_{\mathfrak{X}} = \mathcal{K}^*_{F_m^{(n)}}\big|_{\mathfrak{X} \subset X_m^{(n-1)} \subset F_m^{(n)}}$$

is the restriction to $\mathfrak{X} := {}^\sharp X_m^{(n-2)} \subset X_m^{(n-1)} \subset F_m^{(n)}$ of the anticanonical sheaf of $F_m^{(n)}$, a section of which defines $X_m^{(n-1)} \subset F_m^{(n)}$, so $\mathcal{K}^*_{X_m^{(n-1)}} = \mathcal{O}_{X_m^{(n-1)}}$.

---

[3]With a total degree $\binom{1}{-m}$ and poles of order ℓ at $y_0 = 0$ and $m-\ell$ at $y_1 = 0$ with $\ell \in [1, m-1]$, such monomials cannot be split into sums of two partial fractions (nor any change of variables), each with a single pole.

[4]We thank James Gray for confirming this detail.

In fact, both S_m and C_m are *quasi-Fano* by the n-dimensional generalization of definition [35, Def. 2.2]: They both contain the smooth codimension-2 $^{\sharp}X_m^{(n-2)}$, and their structure sheaf cohomology vanishes except $H^0 \approx \mathbb{C}$, so $h^q(C_m, \mathcal{O}) = \delta_{q,0} = h^q(S_m, \mathcal{O})$, reproducing the defining property, $\chi(\mathcal{O}_{C_m}) = 1 = \chi(\mathcal{O}_{S_m})$; see Appendix A.3. The mirror-pair constructions below, in §3.3, should then provide a testing ground for the so-called *DHT conjecture* [40–46].

3.2. Laurent deformations and intrinsic limit

Since the entire anticanonical system (2.16), i.e., (2.19) factorizes for $m \geqslant 3$, the necessarily Tyurin-degenerate Calabi-Yau hypersurfaces $X_m^{(n-1)} \subset F_m^{(n)}$ in the *central* Hirzebruch scroll (2.1), i.e., (2.13) cannot be smoothed by regular deformations. However, the rational sections encoded by the *extended* Newton polytope [5] make the anticanonical system of $F_m^{(n)}$ transverse, and so afford a Laurent smoothing of $X_m^{(n-1)} \subset F_m^{(n)}$. The simple, $n=2$ case in Figure 4 certainly suggests that the singularity *should have* a *crepant* smoothing, i.e., without changing the (vanishing) canonical class.

Laurent deformations. The Calabi-Yau models in [5] deform the reducible hypersurface (3.3) by including certain very specific rational monomials in the defining section (2.16), i.e., (2.19). Suffice it here to showcase the $X_3^{(1)} \subset F_3^{(2)}$ example in its toric rendition, and focus on the cornerstone (extremal) polynomial

$$(3.11) \qquad f(x; a) = a_1 x_1^2 x_3^5 + a_2 x_1^2 x_4^5 + a_3 \frac{x_2^2}{x_4} + a_4 \frac{x_2^2}{x_3} \quad \in \ \Gamma(\mathcal{K}_{F_3^{(2)}}^*).$$

This particular choice of rational monomials will be explained below; see (3.28). Identifying $F_3^{(2)}$ with the MPCP-desingularization of $\mathbb{P}_{(3:1:1)}^2$ prepends $x_1 \simeq \lambda^0 x_1$ to $(x_2, x_3, x_4) \simeq (\lambda^3 x_2, \lambda x_3, \lambda x_4)$. Thus, (x_1, x_2) are the homogeneous coordinates of the exceptional $\mathbb{P}^1$, so identified by the $(x_1, x_2, x_3, x_4) \simeq (\tilde{\lambda}^1 x_1, \tilde{\lambda}^1 x_2, x_3, x_4)$ symmetry. These two $\mathbb{C}^*$-rescalings are equivalent to the $n=2$, $m=3$ case of (2.13).

While $a_1 a_4^5 \neq a_2 a_3^5$, the polynomial (3.11) is transverse: The gradient $\partial_i f(x; a)$ cannot vanish without setting $x_1 = 0 = x_2$ — which cannot happen in the exceptional $\mathbb{P}^1$ in $F_3^{(2)}$. In the toric specification (2.13), the 1-cones ν_1, ν_2 do not form a 2-cone in $\Sigma_{F_3^{(2)}}$, $\langle x_1 x_2 \rangle$ is in the Stanley-Reisner ideal, and the exceptional set

$$(3.12) \qquad Z(\Sigma_{F_3^{(2)}}) = \{x_1 = 0 = x_2\} \times \mathbb{C}_{x_3, x_4}^2 \cup \mathbb{C}_{x_1, x_2}^2 \times \{x_3 = 0 = x_4\}$$

is excised from $F_3^{(2)} = (\mathbb{C}^4 \smallsetminus Z(\Sigma_{F_3^{(2)}}))/(\mathbb{C}^*)^2$ [15]. (Parts of this base locus *are included,* appropriately and self-consistently, in the Landau-Ginzburg and the so-called hybrid phases of the GLSM model [5].) For this same reason, $x_2 \neq 0$ and so $f(x;a) \neq 0$ at $\{x_1 = 0\}$, so that

$$(3.13) \qquad (S_m = \{x_1 = 0\}) \cap \{f(x;a) = 0\} = \varnothing.$$

For any $a_3, a_4 \neq 0$, the zero-locus $\{f(x;a) = 0\}$ is moved away from the directrix, and thus also from the singular set (3.6). This effectively smoothes the Tyurin-degenerate model, as illustrated in the series of plots in Figure 5, where $a_3 \to \epsilon$ and $a_4 \to 0$, and an additional regular monomial $(x_1 x_2 x_3^2)$ is added,

$$(3.14) \qquad f(x;a) \rightsquigarrow F(x;\epsilon) = x_1^2 x_3^5 + x_1^2 x_4^5 - x_1 x_2 x_3^2 + \epsilon \frac{x_2^2}{x_4},$$

to allow for real solutions in the real $(S^1 \times S^1)$ "slice" within $\mathbb{P}^1_{\text{fibre}} \hookrightarrow F_3^{(2)} \twoheadrightarrow \mathbb{P}^1_{\text{base}}$. Already for $\epsilon = \frac{1}{40}$, the red-plotted slice segment is visi-

(a) $\epsilon = 0$ (b) $\epsilon = \frac{1}{40}$ (c) $\epsilon = \frac{1}{6}$
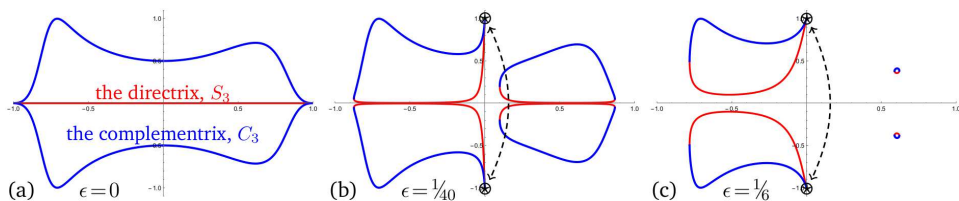
Figure 5: Several plots of $x_1^2 x_3^5 + x_1^2 x_4^5 - x_1 x_2 x_3^2 + \epsilon \frac{x_2^2}{x_4} = 0$, restricted to the real circles $x_1 \to y \in [-1, 1 \simeq -1]$, $x_2 \to \sqrt{1 - y^2}$, $x_3 \to \sqrt{1 - x^2}$ and $x_4 \to x \in [-1, 1 \simeq -1]$; $\{y = 0\}$ is the directrix, $\{x = 0\}$ is the pole-locus; the putative pole-in-zero-locus at $(x, y) = (0, \pm 1)$, filled by the intrinsic limit (below), is marked by the ⊗ symbol

bly deformed away from the directrix, $S_3 = \{x_1 = 0\}$ (the horizontal mid-line in Figure 5), and this separation only increases as ϵ does. In turn, the presence of the rational deformations (3.11) includes a $\frac{0}{0}$-like putative pole in the defining section, which requires special attention.

Intrinsic limit. The main concern with a Laurent defining polynomial such as (3.14) is that the *unqualified* limits of the rational terms, $\lim_{x_3 \to 0} \frac{x_2^2}{x_3}$ and $\lim_{x_4 \to 0} \frac{x_2^2}{x_4}$, are not well defined. The zero-locus of the defining equation at hand is of course well defined away from the putative pole-location,

$\{x_4{=}0\}\cup\{x_3{=}0\}$, which then defines the required qualification: approach the putative pole-locations from *within* the desired zero-locus, thus defining the *intrinsic limit*. For the case at hand, $\{F(x;\epsilon){=}0\}$ with (3.14), we solve:

$$(3.15) \quad F(x;\epsilon)=0, \quad x_4\neq 0 \;\Rightarrow\; x_2 = x_1\frac{x_4x_3^2 \pm \sqrt{x_4}\sqrt{x_4x_3^4 - 4\epsilon(x_3^5 + x_4^5)}}{2\epsilon}.$$

Substituting this in $F(x;\epsilon)$ but keeping the summands separately produces

$$(3.16) \quad 0{=}F(x;\epsilon) = x_1^2x_3^5+x_1^2x_4^5-x_1^2x_3^2\frac{x_4x_3^2\pm\sqrt{x_4}\sqrt{x_4x_3^4-4\epsilon(x_3^5+x_4^5)}}{2\epsilon}$$
$$+x_1^2\frac{\left(x_3^2\sqrt{x_4}\pm\sqrt{x_4x_3^4-4\epsilon(x_3^5+x_4^5)}\right)^2}{4\epsilon},$$
$$\xrightarrow{x_4\to 0} x_1^2x_3^5 + 0 - 0 + (-x_1^2x_3^5),$$

making it clear that each monomial is seprately well defined in the so qualified $x_4{\to}0$ limit. Effectively, the a priori independent (Cox) variable x_2 is replaced with the function $x_2{=}x_2(x_1, x_3, x_4)$ that guarantees the vanishing of $F(x;\epsilon)$ everywhere, including the intersection of this subspace with the pole-locus of concern, $\{x_4{=}0\}$. In this sense, the evaluation of the limit of the rational summand

$$(3.17) \qquad \lim_{x_4\to 0}\left[\epsilon\frac{\left(x_2{=}x_2(x_1,x_3,x_4)\right)^2}{x_4}\right] = -x_1^2x_3^5$$

is an application of L'Hopital's rule, and extends straightfowardly to poles of higher order.

　　With the so-resolved putative pole-locus and at least as real manifolds, we expect the transversal Laurent deformation (3.11) of the Tyurin degeneration (3.3) to be no different than other nonsingular models in the deformation family $\left[\begin{smallmatrix}\mathbb{P}^n\\\mathbb{P}^1\end{smallmatrix}\middle\|\begin{smallmatrix}1\\m\end{smallmatrix}\middle|\begin{smallmatrix}n\\2-m\end{smallmatrix}\right]$, built over the effectively discrete family $\left[\begin{smallmatrix}\mathbb{P}^n\\\mathbb{P}^1\end{smallmatrix}\middle\|\begin{smallmatrix}1\\m\end{smallmatrix}\right]$ in Figure 2. These Laurent-deformed Calabi-Yau models are then expected to have the same Betti and Euler numbers, $b_2{=}2$, $b_3{=}174$ and $\chi{=}{-}168$, and then also to admit a Hodge decomposition with $h^{11}{=}2$ and $h^{21}{=}86$. However, we are not aware of a rigorous proof — or correction.

Alternative.　　The additional care required to specify the nature of the limit-points such as $x_4{\to}0$ in the zero-locus of the Laurent defining function (3.14) stems from the fact that the pole-locus of concern, $\{x_4{=}0\}$, intersects the zero-locus of interest, $\{F(x) = 0\}$. This situation is amenable to the following sequence of standard algebro-geometric operations:

Procedure 1. *For a Laurent polynomial $F(x)$ such as (3.14) over an ambient space A, let $P \subset A$ denote the pole-locus of $F(x)$, $Z \subset A$ the well-defined open (non-compact) zero-locus of $F(x)$, and let x_* be a common point of (limiting sequences in) P and Z. Then:*

    1) Let $\widehat{A}$ be a blowup of A at x_*, possibly iterated so the closure of $\widehat{Z}$, identified as the zero-locus $\{\widehat{F}(x) = 0\} \subset \widehat{A}$, is well defined and separate from the proper transform of the pole-locus, $\widehat{P}$.

    2) The blowdown (along $\hat{x}_*$) of the zero-locus $\{\widehat{F}(x) = 0\} \subset \widehat{A}$ is then a well-defined subspace of A.

(3.18)
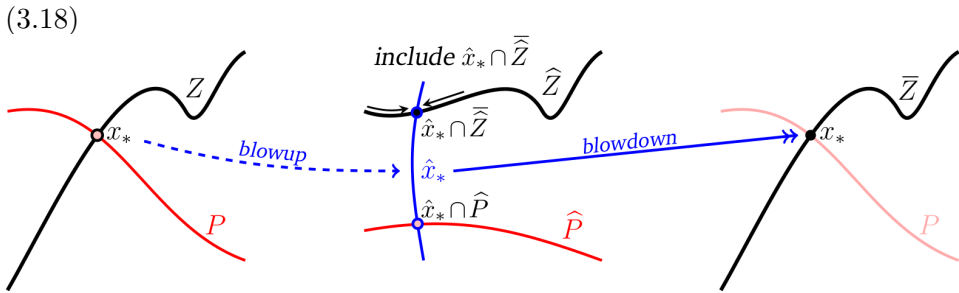
This separates the limiting sequences within the zero-locus from those within the pole-locus, and so conceptually corroborates the above-defined *intrinsic limit*. It also seems to suggest a reformulation wherein coincident points are separated based on limiting sequences that lead to them, perhaps not too dissimilar from the framework of Ref. [4].

An overview. In the footsteps of § 2.5, consider the triply deformed 4-fold

$$(3.19) \qquad \begin{bmatrix} \mathbb{P}^4 \,\big\|\, 1 \\ \mathbb{P}^1 \,\big\|\, 5 \end{bmatrix} \ni \quad x_0\, y_0^{\,5} + x_1\, y_1^{\,5} + x_2\, y_0^{\,4}\, y_1 + x_3\, y_0^{\,3}\, y_1^{\,2} + x_4\, y_0^{\,2}\, y_1^{\,3} = 0,$$

which admits a collection of one degree-$\left(\begin{smallmatrix} 1 \\ -2 \end{smallmatrix}\right)$ and *three* algebraically independent degree-$\left(\begin{smallmatrix} 1 \\ -1 \end{smallmatrix}\right)$ directrices. Via the analogous constant-Jacobian change of variables, this leads to the toric $F^{(4)}_{(2,1,1,1)} \approx_{\mathbb{R}} F^{(4)}_{(1,0,0,0)}$. For each $n \geqslant 2$, $F^{(n)}_{(1,0,\cdots)}$ is Fano: both its spanning and its Newton polytope is convex and reflexive.

So, (2.2) is an explicitly constructed deformation family that includes both Fano and non-Fano Hirzebruch scrolls, all of which (for any given n, m) are diffeomorphic to each other. This then induces a deformation *connection* between the (*secondary* deformation families of) respective Calabi-Yau

hypersurfaces, such as:

(3.20)

$$\underbrace{\overbrace{F^{(4)}_{(1,0,0,0)}[c_1]}^{\text{smooth}} \xleftarrow{q=0} F^{(4)}_{(1,0,0,0)}}_{\text{generic}} \xrightarrow{\;\epsilon\to 0\;} \underbrace{F^{(4)}_{(5,0,0,0)} \xleftarrow{q=0} \overbrace{F^{(4)}_{(5,0,0,0)}[c_1]}^{\text{Tyurin-degenerate}}}_{\text{central}} \supset \overbrace{\mathrm{Sing}\big(X^{(3)}_{(5,0,0,0)}\big)}^{\text{matryoshka}}$$
$$\sharp X^{(2)}_{(5,0,0,0)} = \mathrm{K3}$$

The (irreducible) degree-$\left(\begin{smallmatrix}1\\-5\end{smallmatrix}\right)$ directrix in the central Hirzebruch scroll $F_5^{(n)}$ thus serves as an *obstruction* to regular smoothing of the Tyurin-degenerate Calabi-Yau hypersurface, which disappears away from the central scroll. That is, we have the same real 8-dimensional manifold on the two sides of the $\epsilon\to 0$ arrow, equipped however with discretely different complex structures:

1) The anticanonical sections that are holomorphic with respect to a generic choice of the complex structure are transverse and can define smooth Calabi-Yau hypersurfaces.

2) The anticanonical sections that are holomorphic with respect to the central choice of the complex structure factorize and can define only Tyurin-degenerate Calabi-Yau hypersurfaces.

That is, there always exist smooth defining equations of the correct degree to define a smooth and Ricci-flat zero locus, they are just not holomorphic with respect to the choice of the complex structure in which the smooth directrix is also holomorphic. It is then tempting to conclude:

Conjecture 1. *The Laurent deformations of the Calabi-Yau hypersurface in the central Hirzebruch scroll are $\epsilon\to 0$ limit-images of the regular smoothing deformations in the Calabi-Yau hypersurface within the generic Hirzebruch scrolls.*

3.3. Mirror pairs

We now turn to our primary motivation, the Laurent generalization of the transposition mirror model construction [7–9] and Batyrev's toric construction [10]; see also [11] and references therein.

Transpose mirror. The standard anticanonical *cornerstone* polynomial of $F_3^{(2)}$ (green outline in Figure 6, below),

(3.21)
$$\begin{aligned} x_1^2 x_3^5 &+ x_1^2 x_4^5 + x_1 x_2 x_3^2 + x_1 x_2 x_4^2 \\ &= x_1\big(x_1 x_3^5 + x_1 x_4^5 + x_2 x_3^2 + x_2 x_4^2\big), \end{aligned}$$

is not transverse, but its Laurent analogue [5],

$$(3.11') \qquad f(x) = a_1 x_1^2 x_3^5 + a_2 x_1^2 x_4^5 + a_3 \frac{x_2^2}{x_4} + a_4 \frac{x_2^2}{x_3}, \quad a_1 a_4^5 \neq a_2 a_3^5,$$

is transverse away from the indicated discriminant locus. The matrix of exponents of (3.11) is

$$(3.22) \quad \mathbb{E}[f(x)] = \begin{bmatrix} 2 & 0 & 5 & 0 \\ 2 & 0 & 0 & 5 \\ 0 & 2 & 0 & -1 \\ 0 & 2 & -1 & 0 \end{bmatrix}, \quad \det \mathbb{E}[f(x)] = 0, \quad \operatorname{rank} \mathbb{E}[f(x)] = 3,$$

so that (3.11) is *not invertible* in the sense defined in [9] (see also [47, 48]), which would seem to prevent constructing the mirror model. Nevertheless, the transpose [5, 7] of the defining equation (3.11) is straightforward:

$$(3.23) \quad f(x)^{\mathsf{T}} = g(y) = b_1 y_1^2 y_2^2 + b_2 y_3^2 y_4^2 + b_3 \frac{y_1^5}{y_4} + b_4 \frac{y_2^5}{y_3}, \quad b_1^5 \neq b_2 b_3^2 b_4^2,$$

and is homogeneous for continuously[5] many choices of y_i-degrees:
(3.24)
$$\deg[g(y)] = 1 \implies q(y_1) = \tfrac{1}{5} + \tfrac{1}{5} q(y_4), \quad q(y_2) = \tfrac{3}{10} - \tfrac{1}{5} q(y_4), \quad q(y_3) = \tfrac{1}{2} - q(y_4),$$

all of which automatically satisfy the Calabi-Yau condition, $\sum_{j=1}^{4} q(y_j) = 1$. Choosing a rational value for $q(y_4)$ and clearing denominators, one finds suitable linearly independent 4-vectors $Q(y_i)$, reconstructs the fan of the toric space for which $g(y)$ in (3.23) is an anticanonical section, and then refines[6] the choice of $Q(y_i)$ to proper Mori vectors [29]. To this end:

$$(3.25) \qquad \left. \begin{array}{l} q(y_4) = -1 \\ q(y_4) = \tfrac{3}{2} \end{array} \right\} \implies \begin{bmatrix} \widetilde{Q}^1(y_i) \\ \widetilde{Q}^2(y_i) \end{bmatrix} = \begin{bmatrix} 1 & 0 & -2 & 3 \\ 0 & 1 & 3 & -2 \end{bmatrix}$$

$$\implies \begin{bmatrix} 1 & 0 & -2 & 3 \\ 0 & 1 & 3 & -2 \end{bmatrix} \cdot \begin{bmatrix} -3 & 2 \\ 2 & -3 \\ 0 & 1 \\ 1 & 0 \end{bmatrix} \overset{(2.14)}{=} 0 \quad \overset{\star}{\rightsquigarrow} \quad \begin{bmatrix} -1 & -1 \\ -1 & 4 \\ 1 & -2 \\ 1 & -0 \end{bmatrix}$$

---

[5]This continuousness of scaling symmetry choices correlates with the reduced rank of the matrix of exponents (3.22).

[6]The procedure in [29] yields more than two 4-vectors. Among these, we selects the two of which integral linear combinations reproduce all others. For brevity, we display only this final choice. In turn, the columns formed from the components of this pair of 4-vectors $Q(y_i)$ are 2-vectors with co-prime components; see (3.27).

where $\widetilde{Q}^1(y_j) = 2\,q(y_j)|_{q(y_4)=-1}$ and $\widetilde{Q}^2(y_j) = 2\,q(y_j)|_{q(y_4)=\frac{3}{2}}$ are linearly in-
dependent integral choices. The null-space of their matrix-stack is spanned
by $\widetilde{\mu}_j^1 = (-3, 2, 0, 1)$ and $\widetilde{\mu}_j^2 = (2, -3, 1, 0)$, given in the two columns of the
2×4 right-hand side (blue) matrix in the middle. These two 4-vectors, $\widetilde{\mu}_j^\kappa$ for
$\kappa = 1, 2$, define via the $\star$-labeled arrow (3.25) the final 4-vectors, $\mu_j^1 = \widetilde{\mu}_j^1 + \widetilde{\mu}_j^2$
and $\mu_j^2 = -\widetilde{\mu}_j^1 - 2\widetilde{\mu}_j^2$, given here by the columns of the right-most matrix
in (3.25). Each of these pairs of 4-vectors, $\widetilde{\mu}_j^\kappa$ and μ_j^κ, defines a 4-tuple of
2-vectors, for which the $\star$-labeled transformation (3.25) is simply a $\mathrm{GL}(2; \mathbb{Z})$
basis change:

$$(3.26) \quad \left.\begin{matrix} \mu_j^1 = \widetilde{\mu}_j^1 + \widetilde{\mu}_j^2 \\ \mu_j^2 = -\widetilde{\mu}_j^1 - 2\widetilde{\mu}_j^2 \end{matrix}\right\} \Rightarrow$$

$$\begin{bmatrix} 1 & 1 \\ -1 & -2 \end{bmatrix} \cdot \left[\begin{array}{c|c|c|c} -3 & 2 & 0 & 1 \\ 2 & -3 & 1 & 0 \end{array}\right] \stackrel{*}{=} \left[\begin{array}{c|c|c|c} -1 & -1 & 1 & 1 \\ -1 & 4 & -2 & -1 \end{array}\right]$$

Using this last 4-tuple of 2-vectors as generators of a fan we have, akin
to (2.13):
(3.27)
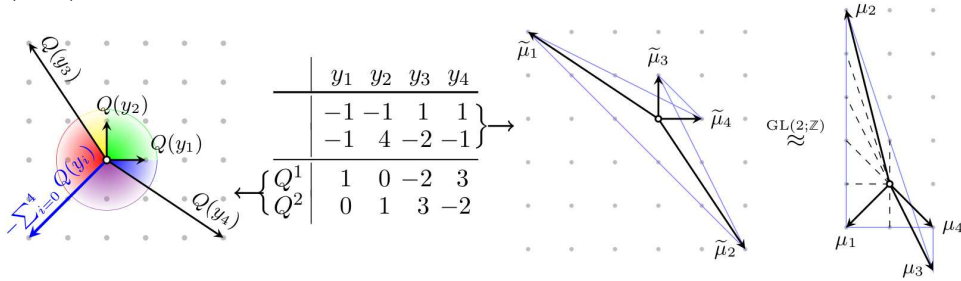
The secondary fan (far left) was read from the columns of the $\widetilde{Q}$-matrix
in (3.25); the corresponding tabulated toric specification and fan generators
on the right are read from the indicated columns in (3.26). The blue line links
the $\widetilde{\mu}$- and μ-vertices in their order determined by (3.25) and (3.26), and the
result outlines precisely the self-crossing polygon that is the *transpolar* [5]
(roughly, iteratively face-wise polar (2.17)) of the non-convex VEX polygon
that spans the $\Sigma_{F_3^{(2)}}$ fan:

(3.28)
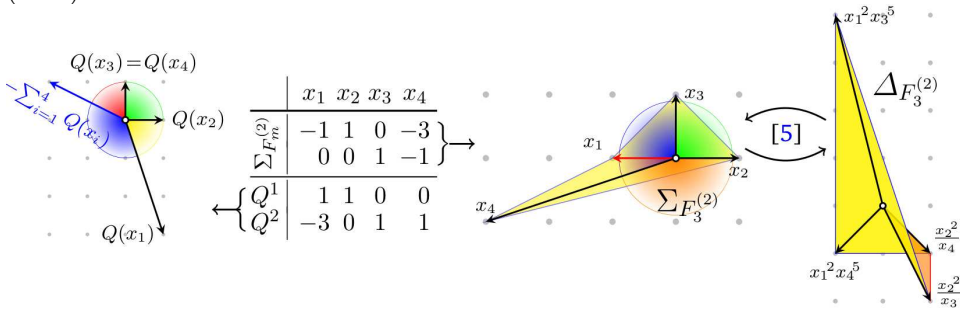
The flip-folded polygon at the right-hand side of both (3.27) and (3.28) spans a *multifan* that, with the dashed unit-degree subdivisions, specifies a smooth toric space in much the same way as does the fan $\Sigma_{F_3^{(2)}}$, depicted mid-right in (3.28)[5, 49, 50].

Toric précis.   The foregoing then demonstrates that the straightforward generalization [5] of the transposition mirror models [7–9] illustrated in Figure 6 for $F_3^{(2)}[c_1]$ and its mirror, where "$\Delta_V^\star \geqslant \Sigma_V$" means that the polytope
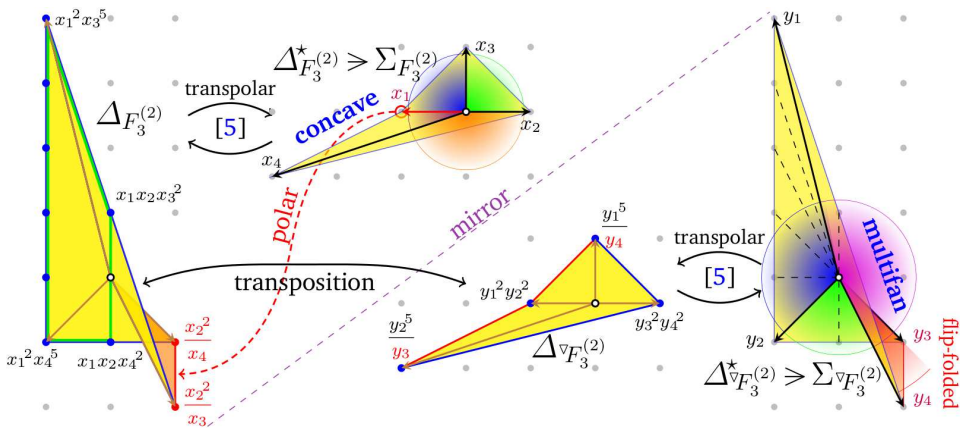
Figure 6: The transpolar pair of VEX polygons used in transposition-mirror fashion: one to define the Cox variables, the other to define anticanonical monomials — and then the other way around

(multitope) $\Delta_V^\star$ spans the (multi)fan Σ_V, i.e., Σ_V star-subdivides $\Delta_V^\star$. The

evident relations

$$(3.29) \qquad \Sigma_{F_3^{(2)}} \lessdot \Delta^\star_{F_3^{(2)}} = \Delta_{\triangledown F_3^{(2)}} \xleftrightarrow[\text{[5]}]{\triangledown} \Delta_{F_3^{(2)}} = \Delta^\star_{\triangledown F_3^{(2)}} \gtrdot \Sigma_{\triangledown F_3^{(2)}}$$

provide the unit-subdivided (multi)fans, $\Sigma_{F_3^{(2)}}$ and $\Sigma_{\triangledown F_3^{(2)}}$, which specify the atlas of smooth local charts for the *ambient* toric spaces, $F_3^{(2)}$ and $\triangledown F_3^{(2)}$, respectively, as each others' *transpolar* toric space. Also, the Cox (homogeneous) variables, displayed in the column-heading rows in (3.28) and (3.27), were used to express the polynomials (3.11) and (3.23), respectively:

$$(3.30a) \qquad g(y)^\mathsf{T} = f(x) = a_1 x_1^2 x_3^5 + a_2 x_1^2 x_4^5 + a_3 \frac{x_2^2}{x_4} + a_4 \frac{x_2^2}{x_3}$$

$$= \sum_{\mu_j \lessdot \Delta_{F_3^{(2)}}} a_j \prod_{\nu_i \lessdot \Delta^\star_{F_3^{(2)}}} x_i^{\langle \mu_j, \nu_i \rangle + 1};$$

$$(3.30b) \qquad f(x)^\mathsf{T} = g(y) = b_1 y_1^2 y_2^2 + b_2 y_3^2 y_4^2 + b_3 \frac{y_1^5}{y_4} + b_4 \frac{y_2^5}{y_3}$$

$$= \sum_{\nu_i \lessdot \Delta^\star_{F_3^{(2)}}} b_i \prod_{\mu_j \lessdot \Delta_{F_3^{(2)}}} y_j^{\langle \mu_j, \nu_i \rangle + 1},$$

where the symbol "$\lessdot$" stands for "is a vertex of" the polytope, i.e., a 1-cone generator of the fan spanned by that polytope. This generalizes the transposition prescription [7–9] and [10], in Cox variables [32], to transpolar pairs of VEX polytopes [5].

For all $n \geqslant 2$ and $m \geqslant 3$, the fan $\Sigma_{F_m^{(n)}}$ is spanned by a non-convex polytope, $\Delta^\star_{F_m^{(n)}}$, reflecting that $F_m^{(n)}$ is not Fano. In turn, the transpolar polytope $\Delta_{F_m^{(n)}}$ is flip-folded and spans a multifan $\Sigma_{\triangledown F_m^{(n)}}$, which when unit-subdivided encodes $\triangledown F_m^{(n)}$ as a (smooth) *toric manifold* [49, 50].

Laurent deformations rationale. The specific choice of the rational monomials included as Laurent deformations of the anticanonical sections, such as in (3.11), is then specified by the following:

- As indicated (red-ink dashed arrow) in Figure 6, the rational monomials, $\left\{ \frac{x_2^2}{x_4}, \frac{x_2^2}{x_3} \right\}$, form the flip-folded edge in $\Delta_{F_3^{(2)}}$, which is polar to the concave (MPCP-desingularizing [10]) vertex $\nu_1 \in \Delta^\star_{F_3^{(2)}}$. The Cox variables in the denominators are defined by the vertices delimiting the concavity in $\Delta^\star_{F_3^{(2)}}$.
- Through the looking glass, the rational monomials $\left\{ \frac{y_1^5}{y_4}, \frac{y_2^5}{y_3} \right\}$ correspond to vertices that delimit the concavity in $\Delta_{\triangledown F_3^{(2)}}$, and the Cox variables in their denominators are defined by vertices that form the flip-folded edge in $\Delta^\star_{\triangledown F_3^{(2)}}$, the one that is polar to the non-convex vertex in $\Delta_{\triangledown F_3^{(2)}}$.

Thus, the rational monomials included both in (3.30a) and in (3.30b) are precisely those that correspond to the *concave subset* in $\Delta^\star_{F_3^{(2)}} = \Delta_{\triangledown F_3^{(2)}}$ and *flip-folded subset* in $\Delta_{F_3^{(2)}} = \Delta^\star_{\triangledown F_3^{(2)}}$ — precisely the features by which VEX polytopes [5] generalize the by now familiar reflexive polytopes [10, 51]. Such self-crossing polygons have been used to encode *(pre)symplectic* spaces [52], which correlates with mirror symmetry relating complex and symplectic structures [53, 54]; of course, each Calabi-Yau space admits both structures.

Thus, the Newton polygons $\Delta_{F_3^{(2)}}$ and $\Delta_{\triangledown F_3^{(2)}}$ (Figure 6 far left and mid-bottom, respectively), both non-convex but VEX [5], specify the (Laurent-deformed) sections for the defining equation of the Calabi-Yau hypersurfaces:

$$(3.31) \qquad F_3^{(2)}[c_1] \ni \{f(x)=0\} \quad \underset{\text{pair}}{\overset{\text{mirror}}{\longleftrightarrow}} \quad \{g(y)=0\} \in {}^\triangledown F_3^{(2)}[c_1].$$

Incidentally, the *standard* Newton polytope of $F_3^{(2)}$ is highlighted in green in the leftmost illustration in Figure 6 and specifies the non-transverse polynomial (3.21); for a 3-dimensional example, see [5].

The above computations (3.11′)–(3.31) are fairly routine for (convex) reflexive polytopes [10, 51]. With the standard *polar* operation generalized to the transpolar — they continue to also hold for VEX polytopes [5]. In fact, suffice it here to mention that numerous combinatorial formulae generalizing the "12-theorem" [15, Theorem 10.5.10] and various results about Chern and other characteristic classes [31] continue to hold provided all polytopes and (multi)fans are taken with orientation-dependent multiplicity. In turn, the so-called A-discriminants for both the complex structure and the Kähler class moduli, as well as the Yukawa couplings continue to be computable and conform to general mirror symmetry expectations. Details of these results will be reported separately.

Specific mirror models.   Since the polynomials (3.11) and (3.23) and the matrix of exponents (3.22) are not invertible, a direct relation to the original transposition prescription [7–9] is provided by particular complementary reducing deformations of (3.30a) and (3.30b), such as:

$$(3.32) \qquad x_1 \to 1 \ \& \ a_4 \to 0 \ \Rightarrow \ f_R(x) = a_1 x_3^5 + a_2 x_4^5 + a_3 \frac{x_2^2}{x_4};$$

$$(3.33) \qquad b_1 \to 0 \ \& \ y_4 \to 1 \ \Rightarrow \ g_R(y) = b_2 y_3^2 + b_3 y_1^5 + b_4 \frac{y_2^5}{y_3}.$$

This reduces the matrix (3.22) to an invertible 3×3 matrix, and may be depicted in terms of the toric data in Figure 6 as shown in Figure 7. Both diagrams here serve both as Newton polygons (Δ_R and $\Delta_{\triangledown R}$, respectively)
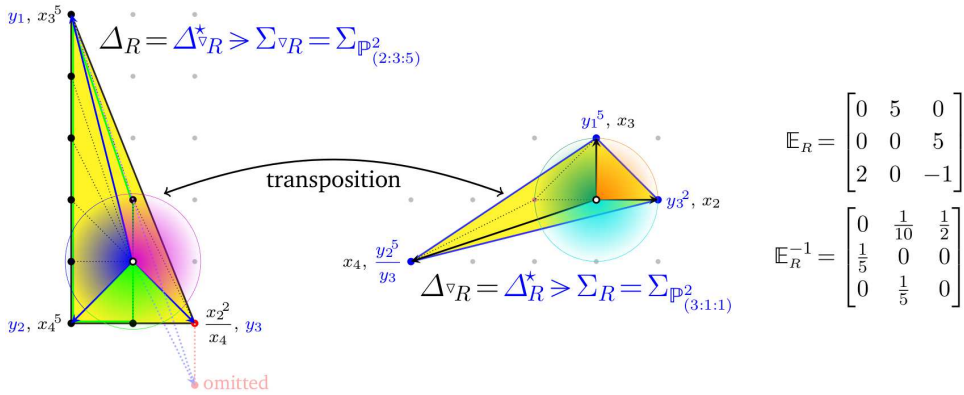
Figure 7: The toric data of the reduced mirror pair (3.32)–(3.33)

with the cornerstone (extreme) monomials indicated, as well as spanning the fans ($\Delta^\star_{\triangledown R} \succ \Sigma_{\triangledown R}$ and $\Delta^\star_R \succ \Sigma_R$, respectively) that identify the Cox variables, and specify the indicated weighted projective spaces identified by the degrees (lattice areas) of the three major cones. Here, $R = \mathbb{P}^2_{(3:1:1)}$ is identified as the blowdown (by un-subdividing at the MPCP-smoothing $\nu_1 = (-1, 0)$ 1-cone generator) of $F_3^{(2)}$. Analogously, $^\triangledown R = \mathbb{P}^2_{(2:3:5)}$ is identifiable as a blowdown of $^\triangledown F_3^{(2)}$ by omitting the $\mu_4 = (1, -2)$ 1-cone generator of the multifan.

Finally, the columns of $\mathbb{E}^{-1}$ specify the discrete symmetries of $f_R(x)$ in (3.32), while its rows analogously pertain to $g_R(y)$ in (3.33) [9]:

$$(3.34) \qquad f_R(x) = a_1 x_3^5 + a_2 x_4^5 + a_3 \frac{x_2^2}{x_4},$$

$$\begin{cases} \mathcal{Q} = \left(\mathbb{Z}_5 : \frac{3}{5}, \frac{1}{5}, \frac{1}{5}\right), \\ \mathcal{G} = \left(\mathbb{Z}_{10} : \frac{1}{10}, 0, \frac{1}{5}\right), \end{cases} \qquad (x_2, x_3, x_4) \in \mathbb{P}^2_{(3:1:1)};$$

$$(3.35) \qquad g_R(y) = b_2 y_3^2 + b_3 y_1^5 + b_4 \frac{y_2^5}{y_3},$$

$$\begin{cases} \widetilde{\mathcal{Q}} = \left(\mathbb{Z}_{10} : \frac{2}{10}, \frac{3}{10}, \frac{5}{10}\right), \\ \widetilde{\mathcal{G}} = \left(\mathbb{Z}_5 : \frac{1}{5}, \frac{1}{5}, 0\right), \end{cases} \qquad (y_1, y_2, y_3) \in \mathbb{P}^2_{(2:3:5)}.$$

The action of the "quantum symmetry" $\mathcal{Q}$ (resp., $\widetilde{\mathcal{Q}}$) on the indicated homogeneous coordinates is specified by the sum of the columns (resp., rows) of $\mathbb{E}^{-1}$, and of course coincides with the (rescaled) weights of $\mathbb{P}^2_{(3:1:1)}$ (resp., $\mathbb{P}^2_{(2:3:5)}$). The action of the "geometric" symmetry is specified by linear combinations of the columns (resp., rows) independent of $\mathcal{Q}$ (resp., $\widetilde{\mathcal{Q}}$), and can

here be chosen to be generated by the 2nd column (resp., 2nd+3rd row) of $\mathbb{E}^{-1}$. The total degree of discrete symmetries being

$$(3.36) \qquad |\mathcal{Q}||\mathcal{G}| = \det[\mathbb{E}] = 50 = |\widetilde{\mathcal{Q}}||\widetilde{\mathcal{G}}|$$

verifies that the $(\mathbb{Z}_5, \mathbb{Z}_{10})$ pair exhausts the options.

The general case.   The above computations are straightforward to follow through for $F_m^{(2)}$, for all m:

$$(3.37a) \qquad f_R(x; m) = a_1 x_3^{m+2} + a_2 x_4^{m+2} + a_3 \frac{x_2^2}{x_4^{m-2}},$$

$$(x_2, x_3, x_4) \in \mathbb{P}^2_{(m:1:1)};$$

$$(3.37b) \qquad g_R(y; m) = b_2 y_3^2 + b_3 y_1^{m+2} + b_4 \frac{y_2^{m+2}}{y_3^{m-2}},$$

$$(y_1, y_2, y_3) \in \mathbb{P}^2_{(2:m:m+2)}.$$

The symmetries depend on the parity of m, but are as straightforward to find from $\mathbb{E}^{-1}$:

$$
\begin{aligned}
\mathcal{Q}(F_m^{(2)}) &= \left(\mathbb{Z}_{m+2} \colon \tfrac{m}{m+2}, \tfrac{1}{m+2}, \tfrac{1}{m+2} \right), \\
(3.38) \quad \mathcal{G}(F_m^{(2)}) &= \begin{cases} \left(\mathbb{Z}_{2(m+2)} \colon \tfrac{m-2}{2(m+2)}, 0, \tfrac{1}{m+2} \right), & m \text{ odd}; \\ \left(\mathbb{Z}_{m+2} \colon \tfrac{m/2-1}{(m+2)}, 0, \tfrac{1}{m+2} \right) \times \left(\mathbb{Z}_2 \colon \tfrac{1}{2}, 0, 0 \right), & m \text{ even} \end{cases}
\end{aligned}
$$

The symmetries of $g_R(y; m)$ are of course flipped:

$$
\begin{aligned}
(3.39) \quad \mathcal{Q}({}^\nabla F_m^{(2)}) &= \begin{cases} \left(\mathbb{Z}_{2(m+2)} \colon \tfrac{1}{m+2}, \tfrac{m}{2(m+2)}, \tfrac{1}{2} \right), & m \text{ odd}; \\ \left(\mathbb{Z}_{m+2} \colon \tfrac{1}{m+2}, \tfrac{m/2}{m+2}, \tfrac{1}{2} \right) \times \left(\mathbb{Z}_2 \colon 0, \tfrac{1}{2}, \tfrac{1}{2} \right), & m \text{ even}; \end{cases} \\
\mathcal{G}({}^\nabla F_m^{(2)}) &= \left(\mathbb{Z}_{m+2} \colon \tfrac{1}{m+2}, \tfrac{1}{m+2}, 0 \right).
\end{aligned}
$$

The total Hilbert space in a Landau-Ginzburg orbifold[55, 56] or the corresponding *phase* of the gauged linear sigma model [17] is a direct sum of the "untwisted" and several "twisted" sectors, which span representations of the "geometric" and "quantum" symmetries, respectively. The hallmark flipped identifications $\mathcal{Q} \approx \widetilde{\mathcal{G}}$ and $\widetilde{\mathcal{Q}} \approx \mathcal{G}$ therefore insure [7] that the "untwisted" and "twisted" sectors of the $f_R(x)$-model match those of the "twisted" and "untwisted" sectors of the $g_R(y)$-model — as required by mirror symmetry.

3.4. Multiple mirrors

The 3-dimensional case was analyzed in some detail in [5] and we adapt some of that specification in Figure 8; see also the display (2.13). Defining the Cox
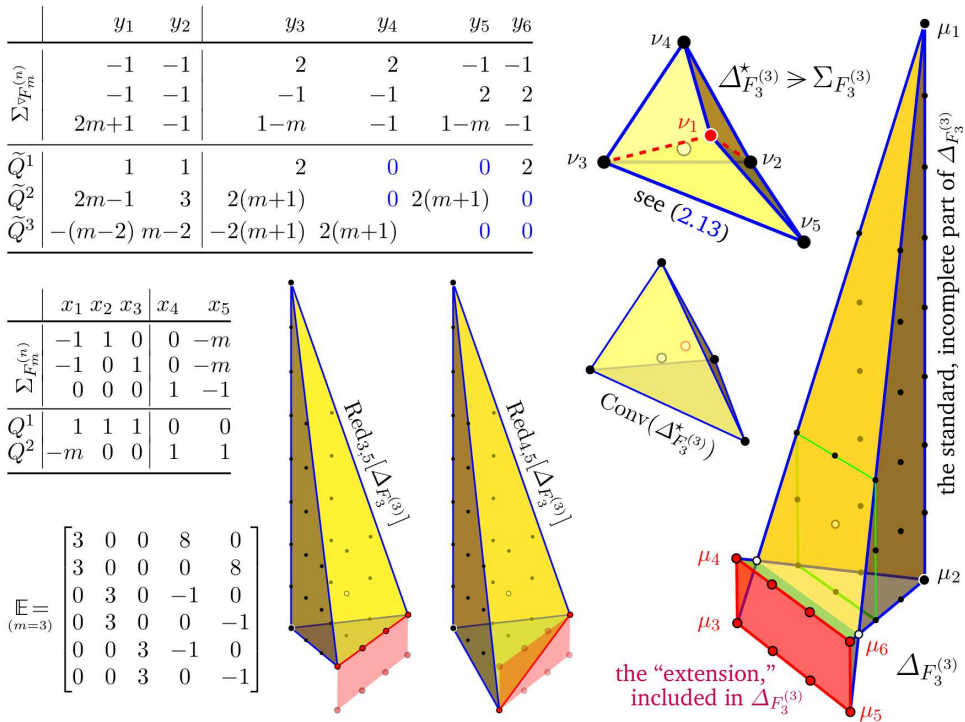
Figure 8: The Newton polytope $\Delta_{F_m^{(3)}}$ specification (top, left), with the $m=3$ case depicted at right; the reduced polytopes are the convex hulls of a minimal subset of the vertices of the original polytope indicated

variables by the vertices of the non-convex polytope $\Delta^\star_{F_m^{(3)}}$ that spans the fan of $F_m^{(3)}$ and limiting to the vertices of the (extended) Newton polytope, $\Delta_{F_m^{(3)}}$, to specify the cornerstone (extremal) monomials — and then the other way around, produces the 3-dimensional analogue of the transposition

mirror pair (3.30):

$$(3.40a) \quad g(y)^\mathsf{T} = f(x) = a_1 \, x_1^3 \, x_4^{2m+2} + a_2 \, x_1^3 \, x_5^{2m+2}$$

$$+ a_3 \, \frac{x_2^3}{x_4^{m-2}} + a_4 \, \frac{x_2^3}{x_5^{m-2}} + a_5 \, \frac{x_3^3}{x_4^{m-2}} + a_6 \, \frac{x_3^3}{x_5^{m-2}},$$

$$(3.40b) \quad f(x)^\mathsf{T} = g(y) = b_1 \, y_1^3 \, y_2^3 + b_2 \, y_3^3 \, y_4^3 + b_3 \, y_5^3 \, y_6^3$$

$$+ b_4 \, \frac{y_1^{2m+2}}{(y_3 \, y_5)^{m-2}} + b_5 \, \frac{y_2^{2m+2}}{(y_4 \, y_6)^{m-2}}.$$

For simplicity, we focus on the $m=3$ case. The 5×6 matrix of exponents is shown in Figure 8 and has rank 4. The bottom-central two diagrams illustrate two inequivalent cornerstone (extremal) reductions of the Newton polytope, whereas only ν_1 may be omitted from $\Delta^\star_{F_3^{(3)}}$ while retaining the origin inside the polytope. This results in two inequivalent, though still extremal, reductions of the matrix of exponents to an invertible 4×4 submatrix. With its many lattice points, the Newton polytope can be reduced in many other ways, leading to a web of mirror models — all "generated" from the transpolar pair $(\Delta^\star_{F_m^{(3)}}, \Delta_{F_m^{(3)}})$.

Mirror-pair #1. The first of these two pairs

$$(3.41a) \quad \left(\operatorname*{Red}_{1;3,5} g(y) \right)^\mathsf{T} = \operatorname*{Red}_{1;3,5} f(x) = a_1 \, x_4^8 + a_2 \, x_5^8 + a_4 \, \frac{x_2^3}{x_5} + a_6 \, \frac{x_3^3}{x_5}$$

$$\in \mathbb{P}^3_{(3:3:1:1)}[8],$$

$$(3.41b) \quad \left(\operatorname*{Red}_{1;3,5} f(x) \right)^\mathsf{T} = \operatorname*{Red}_{1;3,5} g(y) = b_2 \, y_4^3 + b_3 \, y_6^3 + b_4 \, y_1^8 + b_5 \, \frac{y_2^8}{y_4 \, y_6}$$

$$\in \mathbb{P}^3_{(3:5:8:8)}[24],$$

corresponds to $\operatorname{Conv}\left(\Delta^\star_{F_3^{(3)}} \setminus \nu_1 \right)$ and $\operatorname{Conv}\left(\Delta_{F_3^{(3)}} \setminus \{\mu_3, \mu_5\} \right)$. For a generic choice of the coefficients, the polynomials (3.41) are Δ-regular, and are each other's transpose. The so-reduced matrix of exponents is regular:

$$(3.42) \qquad (3.41) \Rightarrow \operatorname*{Red}_{1;3,5} \mathbb{E}(F_3^{(3)}) = \begin{bmatrix} 0 & 0 & 8 & 0 \\ 0 & 0 & 0 & 8 \\ 3 & 0 & 0 & -1 \\ 0 & 3 & 0 & -1 \end{bmatrix},$$

$$\left(\operatorname*{Red}_{1;3,5} \mathbb{E}(F_3^{(3)}) \right)^{-1} = \begin{bmatrix} 0 & \frac{1}{24} & \frac{1}{3} & 0 \\ 0 & \frac{1}{24} & 0 & \frac{1}{3} \\ \frac{1}{8} & 0 & 0 & 0 \\ 0 & \frac{1}{8} & 0 & 0 \end{bmatrix},$$

and the discrete symmetries of the polynomials (3.41) are read off from the inverse matrix:

$$(3.43a) \qquad a_1\, x_4^8 + a_2\, x_5^8 + a_4\, \frac{x_2^3}{x_5} + a_6\, \frac{x_3^3}{x_5} :$$

$$\left\{ \frac{\begin{matrix} \left(\mathbb{Z}_3 \colon \frac{1}{3}, \frac{2}{3}, 0, 0\right) \\ \left(\mathbb{Z}_{24} \colon \frac{1}{24}, \frac{1}{24}, 0, \frac{1}{8}\right) \end{matrix}}{\left(\mathbb{Z}_8 \colon \frac{3}{8}, \frac{3}{8}, \frac{1}{8}, \frac{1}{8}\right)} \begin{bmatrix} x_2 \\ x_3 \\ x_4 \\ x_5 \end{bmatrix} \right. : \qquad \left\{ \frac{\mathcal{G} = \mathbb{Z}_3 \times \mathbb{Z}_{24},}{\mathcal{Q} = \mathbb{Z}_8.} \right.$$

$$(3.43b) \qquad b_2\, y_4^3 + b_3\, y_6^3 + b_4\, y_1^8 + b_5\, \frac{y_2^8}{y_4\, y_6} :$$

$$\left\{ \frac{\begin{matrix} \left(\mathbb{Z}_8 \colon \frac{1}{8}, 0, 0, 0\right) \\ \left(\mathbb{Z}_3 \colon 0, 0, \frac{1}{3}, \frac{2}{3}\right) \end{matrix}}{\left(\mathbb{Z}_8 \colon \frac{5}{24}, \frac{3}{24}, \frac{1}{3}, \frac{1}{3}\right)} \begin{bmatrix} y_1 \\ y_2 \\ y_4 \\ y_6 \end{bmatrix} \right. : \qquad \left\{ \frac{\mathcal{G}^\nabla = \mathbb{Z}_8 \times \mathbb{Z}_3,}{\mathcal{Q}^\nabla = \mathbb{Z}_{24}.} \right.$$

To insure the geometric and quantum symmetry swap, we may consider the models

$$(3.44) \qquad \left((3.43a)/\mathbb{Z}_3 \,, (3.43b) \right) \qquad \text{and} \qquad \left((3.43a)\,, (3.43b)/\mathbb{Z}_3 \right)$$

for two possible mirror pairs, in each case using the traceless $\mathbb{Z}_3$-action indicated in (3.43a) and (3.43b), respectively. Finally, notice the factor "3" in the relation $d(\mathrm{Red}_{3,5}[\varDelta_{F_3^{(3)}}]) = 3d(\varDelta^\star_{\mathbb{P}^3_{(8:8:5:3)}})$, correlating to the order of the $\mathbb{Z}_3$ group in (3.44), which was called H in Ref. [7].

Mirror-pair #2. On the other hand,

$$(3.45a) \quad \left(\underset{1;4,5}{\mathrm{Red}}\, g(y) \right)^{\mathsf{T}} = \underset{1;4,5}{\mathrm{Red}}\, f(x; F_3^{(3)})$$

$$= a_1\, x_4^8 + a_2\, x_5^8 + a_3\, \frac{x_2^3}{x_4} + a_6\, \frac{x_3^3}{x_5} \quad \in\ \mathbb{P}^3_{(3:3:1:1)}[8],$$

$$(3.45b) \quad \left(\underset{1;4,5}{\mathrm{Red}}\, f(x) \right)^{\mathsf{T}} = \underset{1;4,5}{\mathrm{Red}}\, g(y; {}^\nabla F_3^{(3)})$$

$$= b_2\, y_3^3 + b_3\, y_6^3 + b_4\, \frac{y_1^8}{y_3} + b_5\, \frac{y_2^8}{y_6} \quad \in\ \mathbb{P}^3_{(1:1:2:2)}[6],$$

corresponds to $\mathrm{Conv}\left(\varDelta^\star_{F_3^{(3)}} \smallsetminus \{\nu_1\}\right)$ and $\mathrm{Conv}\left(\varDelta_{F_3^{(3)}} \smallsetminus \{\mu_4, \mu_5\}\right)$. For a generic choice of the coefficients, the polynomials (3.45) are again Δ-regular, and are each other's transpose. The so-reduced matrix of exponents is again

regular:

$$(3.46) \qquad (3.45a) \ \& \ (3.45b) \Rightarrow \quad \underset{1;4,5}{\mathrm{Red}}\,\mathbb{E}(F_3^{(3)}) = \begin{bmatrix} 0 & 0 & 8 & 0 \\ 0 & 0 & 0 & 8 \\ 3 & 0 & -1 & 0 \\ 0 & 3 & 0 & -1 \end{bmatrix},$$

$$\left(\underset{1;4,5}{\mathrm{Red}}\,\mathbb{E}(F_3^{(3)}) \right)^{-1} = \begin{bmatrix} \frac{1}{24} & 0 & \frac{1}{3} & 0 \\ 0 & \frac{1}{24} & 0 & \frac{1}{3} \\ \frac{1}{8} & 0 & 0 & 0 \\ 0 & \frac{1}{8} & 0 & 0 \end{bmatrix},$$

and the discrete symmetries of the polynomials (3.41) are read off from the inverse matrix:

$$(3.47) \qquad a_1\,x_4^{\,8} + a_2\,x_5^{\,8} + a_4\,\frac{x_2^{\,3}}{x_5} + a_5\,\frac{x_3^{\,3}}{x_4} :$$

$$\left\{ \frac{\begin{pmatrix} \mathbb{Z}_3 \colon \frac{1}{3}, \frac{1}{3}, 0, 0 \end{pmatrix}}{\begin{pmatrix} \mathbb{Z}_{24} \colon \frac{1}{24}, \frac{23}{24}, \frac{1}{8}, \frac{7}{8} \end{pmatrix}}{\begin{pmatrix} \mathbb{Z}_8 \colon \frac{3}{8}, \frac{3}{8}, \frac{1}{8}, \frac{1}{8} \end{pmatrix}} \begin{bmatrix} x_2 \\ x_3 \\ x_4 \\ x_5 \end{bmatrix} : \quad \left\{ \begin{array}{l} \mathcal{G} = \mathbb{Z}_3 \times \mathbb{Z}_{24}, \\ \overline{\mathcal{Q} = \mathbb{Z}_8.} \end{array} \right. \right.$$

$$(3.48) \qquad b_2\,y_4^{\,3} + b_3\,y_5^{\,3} + b_4\,\frac{y_1^{\,8}}{y_5} + b_5\,\frac{y_2^{\,8}}{y_4} :$$

$$\left\{ \frac{\begin{pmatrix} \mathbb{Z}_4 \colon \frac{1}{4}, \frac{1}{4}, 0, 0 \end{pmatrix}}{\begin{pmatrix} \mathbb{Z}_{24} \colon \frac{1}{24}, \frac{23}{24}, \frac{1}{3}, \frac{2}{3} \end{pmatrix}}{\begin{pmatrix} \mathbb{Z}_6 \colon \frac{1}{6}, \frac{1}{6}, \frac{1}{3}, \frac{1}{3} \end{pmatrix}} \begin{bmatrix} y_1 \\ y_2 \\ y_3 \\ y_6 \end{bmatrix} : \quad \left\{ \begin{array}{l} \mathcal{G}^{\triangledown} = \mathbb{Z}_4 \times \mathbb{Z}_{24}, \\ \overline{\mathcal{Q}^{\triangledown} = \mathbb{Z}_6.} \end{array} \right. \right.$$

The desired swap of "geometric" and "quantum" symmetries can be achieved following [7]: we should consider instead the quotient models $(3.47)/\mathbb{Z}_4$ and $(3.48)/\mathbb{Z}_3$ for a mirror pair. To this end, we may use the $\left(\mathbb{Z}_4 \colon \frac{1}{4}, \frac{3}{4}, \frac{1}{4}, \frac{3}{4} \right)$ generated by the 6-fold difference between the two leftmost columns, and the $\left(\mathbb{Z}_3 \colon \frac{1}{3}, \frac{2}{3}, \frac{2}{3}, \frac{1}{3} \right)$ generated by the 8-fold difference between the two topmost rows in $(\mathrm{Red}_{1;4,5}\,\mathbb{E}(F_3^{(3)}))^{-1}$. For the so-defined models,

$$(3.49) \quad (3.47)/\mathbb{Z}_4 \left\{ \begin{array}{l} \widetilde{\mathcal{G}} = \mathbb{Z}_3 \times \mathbb{Z}_6, \\ \widetilde{\mathcal{Q}} = \mathbb{Z}_8 \times \mathbb{Z}_4; \end{array} \right. \quad \mathrm{vs.} \quad \left. \begin{array}{l} \widetilde{\mathcal{G}}^{\triangledown} = \mathbb{Z}_4 \times \mathbb{Z}_8, \\ \widetilde{\mathcal{Q}}^{\triangledown} = \mathbb{Z}_6 \times \mathbb{Z}_3; \end{array} \right\} (3.48)/\mathbb{Z}_3.$$

Fractional relation. Finally, (3.41b) and (3.45b) are, respectively, transposes of (3.41a) and (3.45a), which are evidently related by deformation — a variation in the coefficient space of the a_I's in (3.40a). It then follows that (3.41b) and (3.45b) should be related by a corresponding, *dual* transformation, in the y_I-space. Indeed, the requisite (*constant-Jacobian*) fractional

change of variables (à la [57–62]) is

$$(3.50) \quad (3.41b): \ \mathbb{P}^3_{(3:5:8:8)} \ni (y_1, y_2, y_4, y_6) \to \left(\frac{y_1}{\sqrt[8]{y_6}}, y_2\sqrt[8]{y_6}, y_4, y_6 \right)$$

$$\mapsto (y_1, y_2, y_4, y_5) \in \mathbb{P}^3_{(1:1:2:2)} \ : (3.45b),$$

which also turns the $\mathbb{Z}_{24}$ $\mathcal{Q}^\nabla$-action from (3.43b) into the $\mathbb{Z}_6$ $\mathcal{Q}^\nabla$-action in (3.48):

$$(3.51)$$

$\underset{1;3,5}{\text{Red}}$	y_1	y_2	y_4	y_6
$\mathbb{Z}_{24}$	$\frac{5}{24}$	$\frac{3}{24}$	$\frac{1}{3}$	$\frac{1}{3}$

$\mapsto$

	$y_1/\sqrt[8]{y_6}$	$y_2\sqrt[8]{y_6}$	y_4	y_6
$\mathbb{Z}_{24}$	$\frac{5-1}{24}$	$\frac{3+1}{24}$	$\frac{1}{3}$	$\frac{1}{3}$

$\simeq$

$\underset{1;4,5}{\text{Red}}$	y_1	y_2	y_4	y_5
$\mathbb{Z}_6$	$\frac{1}{6}$	$\frac{1}{6}$	$\frac{1}{3}$	$\frac{1}{3}$

Since this assignment involves the 8th root, the mapping also involves a $\mathbb{Z}_8$-orbifold quotient, indicating that the models (3.41b) and (3.45b) are birational to each other: they are so-called "multiple mirrors" [63–66].

We take this as further evidence that the wide selection of $K3$ surfaces one can define with the pair of polynomials (3.40), their deformations and after requisite complementary finite quotients as in (3.49), and so ultimately with the transpolar pair of polytopes $\Delta^\star_{F_3^{(3)}}$ and $\Delta_{F_3^{(3)}} = \Delta^\star_{\triangledown F_3^{(3)}}$, indeed form mirror pairs — after appropriate MPCP-desingularization encoded by the unit star-subdivisions. In turn, as shown in §2, this collection stems merely from the central member of the deformation family $\left[\begin{smallmatrix} \mathbb{P}^3 \\ \mathbb{P}^1 \end{smallmatrix} \middle\| \begin{smallmatrix} 1 \\ 3 \end{smallmatrix} \right]$, which leaves many other open avenues for further exploration; see Figure 2.

Tyurin degenerations, again. The straightforward transposition mirror pair of polynomials, such as explicitly given in (3.40) for $F_m^{(3)}$, include rational monomials for $m \geq 3$ and are both transverse.

Consider now the limit in which the rational monomials are omitted. For the anticanonical system of $F_m^{(n)}$ (2.18), this amounts to omitting the extension of the Newton polytope, $\Delta_{F_m^{(n)}}$ (e.g., Figure 8) reducing it at a (green-outlined) new facet that includes the origin. This regular part of the Newton polytope, $\text{reg}[\Delta_{F_m^{(n)}}]$, spans an *incomplete fan* that covers only a half-space; each anticanonical section,

$$(3.52) \qquad \text{reg}[f(x)] = \sum_{\mu \in M \cap \text{reg}[\Delta_{F_m^{(n)}}]} a_\mu \Big(\prod_{\nu_i \prec \Delta^\star_{F_m^{(n)}}} x_i^{\langle \nu_i, \mu \rangle + 1} \Big),$$

$$\text{reg}[\Delta_{F_m^{(n)}}] = \big(\text{Conv}[\Delta^\star_{F_m^{(n)}}] \big)^\circ,$$

factorizes, and has a Tyurin degenerate zero locus. In turn, direct computation shows that the regular part of the transpose of the full Laurent polynomial,

$$(3.53) \qquad \mathrm{reg}\left[f(x)^{\mathsf{T}} = \sum_{\nu \in N \cap \Delta^{\star}_{F_m^{(n)}}} b_\nu \left(\prod_{\mu_i \triangleleft \Delta_{F_m^{(n)}}} y_i^{\langle \mu_i, \nu \rangle + 1} \right) = g(y) \right],$$

does not factorize but fails to be transverse only at isolated points. Finally, the transpose of $\mathrm{reg}[f(x)]$,

$$(3.54) \qquad \left(\mathrm{reg}[f(x)] \right)^{\mathsf{T}} = \sum_{\nu \in N \cap \Delta^{\star}_{F_m^{(n)}}} b_\nu \left(\prod_{\mu'_i \triangleleft \mathrm{reg}[\Delta_{F_m^{(n)}}]} \eta_i^{\langle \mu'_i, \nu \rangle + 1} \right) = g(\eta),$$

consists of the same sections as the complete Laurent $g(y)$, but is re-expressed in terms of the Cox variables η, defined by the vertices of $\mathrm{reg}[\Delta_{F_m^{(n)}}]$. This $g(\eta)$ does not factorize either, but fails to be transverse at a 1-dimensional curve. The increase in the singularity,

$$(3.55) \quad \dim \left[\left\{ \mathrm{d}\, \mathrm{reg}\left[f(x)^{\mathsf{T}} = g(y) \right] = 0 \right\} \right] = 0$$
$$\rightsquigarrow \quad \dim \left[\left\{ \mathrm{d}\left(\mathrm{reg}[f(x)]^{\mathsf{T}} = g(\eta) \right) = 0 \right\} \right] = 1,$$

thus seems to stem from the use of Cox variables that correspond to the incomplete fan $\Sigma' \lessdot \mathrm{reg}[\Delta_{F_m^{(n)}}]$.

For the various deformations of the central Hirzebruch scroll, such as discussed in §2.5, the regular part of the anticanonical systems is less singular. For example, both the generic $\mathrm{reg}[\Delta_{F_{(3,2,\cdots)}^{(n)}}]$-sections and their transposes are transverse. Here, Tyurin degenerations both in the "original" and in the transpose mirror model are smoothable by regular sections. In turn, the generic $\mathrm{reg}[\Delta_{F_{(4,1,\cdots)}^{(n)}}]$-sections have isolated singular points, while their transposes are transverse. Here, Tyurin degenerations of the transpose mirror model is fully smoothable by regular sections, while the singularity of the "original" may be reduced by regular sections to isolated singular points, but needs rational sections for full smoothing.

3.5. Algebro-geometric avenues

The discussion of §3.2 involved the notion of the *intrinsic limit,* which is ostensibly not part of the standard tool-set in algebraic geometry. Although Procedure 1 provides an alternative formulation that involves decidedly more familiar algebro-geometric operations, it seems worth indicating two more alternative formulations of these Laurent models.

Weil divisors.   Consider the $a_i \to 1$ special case of the particular Laurent polynomial (3.34):

$$(3.56) \qquad f_R(x) = x_3^5 + x_4^5 + \frac{x_2^2}{x_4} = \frac{x_3^5 x_4 + x_4^6 + x_2^2}{x_4}, \qquad \in \mathbb{P}^2_{(3:1:1)}[5].$$

The factorization of the regular anticanonical sections (3.1) of $F_m^{(n)}$ for $m \geqslant 3$ implies that their zero-locus (3.3) reduces to a union of two hypersurfaces, i.e., to a sum, $[\mathfrak{c}^{-1}(0)] + [\mathfrak{s}^{-1}(0)]$, of the corresponding divisors. The formal factorization (3.56) analogously corresponds to[7]:

$$(3.57a) \qquad\qquad \left[f_R^{-1}(0)\right] = \left[\{\mathfrak{n}(x)/\mathfrak{d}(x) = 0\}\right] = \left[\mathfrak{n}^{-1}(0)\right] - \left[\mathfrak{d}^{-1}(0)\right],$$

where

$$(3.57b) \qquad\qquad \mathfrak{n}(x) := x_3^5 x_4 + x_4^6 + x_2^2, \qquad \mathfrak{n}^{-1}(0) \in \mathbb{P}^2_{(3:1:1)}[6],$$

$$(3.57c) \qquad\qquad \mathfrak{d}(x) := x_4, \qquad\qquad\qquad \mathfrak{d}^{-1}(0) \in \mathbb{P}^2_{(3:1:1)}[1]$$

are the (sextic) numerator and (linear) denominator divisors in $\mathbb{P}^2_{(3:1:1)}$.

Formal integral *differences* of divisors (in this case, zero-loci of otherwise regular sections) such as (3.57a) are *Weil divisors* [13–15], introduced a century ago as *virtual varieties* by F. Severi [67]. These then provide a standard algebro-geometric framework for the Calabi-Yau zero-locus $f_R^{-1}(0)$ — and in fact all the Laurent-deformed codimension-1 Calabi-Yau models of in non-Fano varieties [5].

Owing to their respective degrees, $\mathfrak{n}(x)$ and $\mathfrak{d}(x)$ differ significantly: Regular sextic polynomials such as $\mathfrak{n}(x)$ on $\mathbb{P}^2_{(3:1:1)}$ freely involve all three quasi-homogeneous coordinates and are sections of the *line bundle* $\mathcal{O}(6)$. By contrast, regular linear polynomials such as the denominator, $\mathfrak{d}(x)$, on $\mathbb{P}^2_{(3:1:1)}$ can involve only the latter two quasi-homogeneous coordinates, x_3, x_4, and are sections of the *sheaf* $\mathcal{O}(1)$. This then implies that $f_R(x)$ also is a section of the $\mathcal{O}(5)$ *sheaf* on $\mathbb{P}^2_{(3:1:1)}$. For most of the physics-motivated computations the precise distinction between sheaves and bundles does not seem to matter in the intended physics applications [19], but the distinction exists and may well be worth a formally more rigorous analysis.

This reformulation (3.57a) of the Laurent model (3.56) as the formal *difference* of two regular divisors (3.57) then opens another avenue of studying such subspaces of well-understood "ambient" spaces, $X \subset A$. Of particular interest are of course methods for computing their numerical characteristics

---

[7]We thank Amin Gholampour for alerting us to this formulation and avenue for further study.

such as the Euler number, Hodge numbers, and then also (topological) intersection numbers of their own divisors and other subspaces, i.e., various Yukawa couplings. It is worth noticing that the contributions of the denominator divisor, $[\mathfrak{d}^{-1}(0)]$, to such numerical characteristics typically *subtract* from those of the numerator divisor, $[\mathfrak{n}^{-1}(0)]$ — and this resonates with the overall structure of results in [5].

Fractional mapping.   Having already seen fractional coordinate changes such as (3.50) above, it is perhaps no surprise that another fractional coordinate change may simplify — indeed, *regularize*[8] — the Laurent defining equation (3.34):

$$(3.34) \qquad f(x) = x_3^5 + x_4^5 + \frac{x_2^2}{x_4} \qquad\qquad (x_2, x_3, x_4) \in \mathbb{P}^2_{(3:1:1)}[5]$$

$$(3.58a) \qquad (x_2, x_3, x_4) \mapsto (z_3\sqrt{z_2}, z_1^2, z_2)$$

$$(3.58b) \qquad h(z) = z_1^{10} + z_2^5 + z_3^2 \qquad\qquad (z_1, z_2, z_3) \in \mathbb{P}^2_{(1:2:5)}[10].$$

This effectively re-renders the Laurent model as a regular algebraic variety — at a price: The indicated mapping[9] involves $\sqrt{z_2}$ and so a double cover that is branched over the $z_2 = 0$ locus; it also maps $x_1 \mapsto z_1^2$ and so involves a $\mathbb{Z}_2$ quotient (with respect to $z_1 \to -z_1$) with the $z_1 = 0$ fixed-point set. This then relates the Calabi-Yau Laurent model $\mathbb{P}^2_{(1:1:3)}[5]$ with the decic hypersurface $\mathbb{P}^2_{(1:2:5)}[10]$ — a variety of *the general-type* $(c_1 < 0)$ — via this $\mathbb{Z}_2$-quotient of a branched double covering map; the reverse mapping is no simpler. While this makes the analysis fairly convoluted (cf. [19, § 5.4–5.5]) it does show that the original Laurent model $\mathbb{P}^2_{(1:1:3)}[5]$ is closely related to a regular algebraic variety, and in a way that involves standard and more familiar algebro-geometric operations.

The mapping (3.58) might appear to be a fortuitous fluke. However, it does have a generalization that is applicable not only to the (rationally extended) anticanonical system of $\mathbb{P}^2_{(3:1:1)}$, but in fact to the entire anticanonical system of $F_3^{(2)}$ from whence (3.34) originally stems, and also extends straightforwardly to higher-twisted Hirzebruch scrolls. Using the toric

---

[8]We are grateful to David Cox for providing this proof-of-concept example and Hal Schenck for communicating it to us.

[9]The direction of the left-hand side dashed arrows in (3.58) and (3.59) follows the coordinate assignment, which is dual — and so of opposite direction of the mapping between the underlying spaces, shown on the right-hand side.

rendition of these monomials, we have:

(3.59a) $f(x) = x_1^2(x_3 \oplus x_4)^5 \;\oplus\; x_1 x_2 (x_3 \oplus x_4)^2 \;\oplus\; x_2^2\left(\frac{1}{x_4} \oplus \frac{1}{x_3}\right)$ $F_3^{(2)}\left[\begin{smallmatrix}2\\-1\end{smallmatrix}\right] = \left[\begin{smallmatrix}\mathbb{P}^2\\\mathbb{P}^1\end{smallmatrix}\middle|\middle|\begin{smallmatrix}1\\3\end{smallmatrix}\middle|\begin{smallmatrix}2\\-1\end{smallmatrix}\right]$

(3.59b) $(x_1, x_2, x_3, x_4) \mapsto (z_1\sqrt{z_3},\, z_2\sqrt{z_3}\, z_4^3,\, z_3,\, z_4)$

(3.59c) $h(z) = z_1^2\left(z_3(z_3 \oplus z_4)^5\right) \;\oplus\; z_1 z_2\left(z_3(z_3 \oplus z_4)^2 z_4^3\right) \;\oplus\; z_2^2\left((z_3 \oplus z_4)\, z_4^5\right)$ $F_0^{(2)}\left[\begin{smallmatrix}2\\6\end{smallmatrix}\right] = \left[\begin{smallmatrix}\mathbb{P}^1\\\mathbb{P}^1\end{smallmatrix}\middle|\middle|\begin{smallmatrix}2\\6\end{smallmatrix}\right],$

(3.59d) $\deg(x_1, x_2, x_3, x_4) = \left(\begin{smallmatrix}1\\-3\end{smallmatrix}, \begin{smallmatrix}1\\0\end{smallmatrix}, \begin{smallmatrix}0\\1\end{smallmatrix}, \begin{smallmatrix}0\\1\end{smallmatrix}\right), \quad \deg(z_1, z_2, z_3, z_4) = \left(\begin{smallmatrix}1\\0\end{smallmatrix}, \begin{smallmatrix}1\\0\end{smallmatrix}, \begin{smallmatrix}0\\1\end{smallmatrix}, \begin{smallmatrix}0\\1\end{smallmatrix}\right)$

While it looks a little more involved than (3.58), the (dash-arrow) mapping (3.59) now also includes (**1**) the hallmark directrix $\{x_1 = 0\} \subset F_3^{(2)}$, and (**2**) the "untwisted" Hirzebruch scroll, $F_0^{(2)}$ — all while staying at the same level of conceptual complexity in mapping the Calabi-Yau subspace: The (presumably desingularized) finite quotient of a branched multiple cover mapping (3.59) relates the Calabi-Yau hypersurface (2-torus) $X_3^{(1)} \subset F_3^{(2)}$ in the non-Fano Hirzebruch scroll $F_3^{(2)}$ (a 3-twisted $\mathbb{P}^1$-bundle over $\mathbb{P}^1$) to a regular degree-$\left(\begin{smallmatrix}2\\6\end{smallmatrix}\right)$ hypersurface in $F_0^{(2)} = \mathbb{P}^1 \times \mathbb{P}^1$ (the "untwisted" plain product), which is of (semi-)general type: $c_1 = 0$ over one $\mathbb{P}^1$-factor, but $c_1 < 0$ over the other.

This "un/twisting" fractional mapping (see footnote 9) between $F_0^{(2)}$ and $F_3^{(2)}$ is most definitely *not* the classical diffeomorphism, $F_m^{(n)} \approx_{\mathbb{R}} F_{m\,(\mathrm{mod}\,n)}^{(n)}$. Also, we note that this (dash-arrow) mapping of defining polynomials is injective but most definitely not surjective: only 10 of the 21 monomials from the full deformation family $\left[\begin{smallmatrix}\mathbb{P}^1\\\mathbb{P}^1\end{smallmatrix}\middle|\middle|\begin{smallmatrix}2\\6\end{smallmatrix}\right]$ turn up in the image (3.59c). That is, this (dash-arrow) mapping exists only over the special subset in the full deformation family $\left[\begin{smallmatrix}\mathbb{P}^1\\\mathbb{P}^1\end{smallmatrix}\middle|\middle|\begin{smallmatrix}2\\6\end{smallmatrix}\right]$, specified by the particular degree-$\left(\begin{smallmatrix}2\\6\end{smallmatrix}\right)$ polynomials (3.59c). Qualitatively, this reminds of the situation illustrated in Figure 2. While more precise details of such mappings are needed to effectively compute numerical characteristics of Laurent models in general, suffice it here to establish their existence and state their general nature.

Infinite pools of constructions. The numerator divisor, $\left[\mathfrak{n}^{-1}(0) \in \mathbb{P}^2_{(3:1:1)}[6]\right]$ in (3.57), has a negative 1st Chern class, and so is a subvariety of *general type,* as is the regular variety, $\mathbb{P}^2_{(1:2:5)}[10]$, in (3.58). More generally, such "regularizing" mappings involve a variety with a *partially negative* 1st Chern class: for $F_0^{(2)}\left[\begin{smallmatrix}2\\6\end{smallmatrix}\right] = \left[\begin{smallmatrix}\mathbb{P}^1\\\mathbb{P}^1\end{smallmatrix}\middle|\middle|\begin{smallmatrix}2\\6\end{smallmatrix}\right]$ in (3.59c), c_1 vanishes over the first (upper) $\mathbb{P}^1$-factor and is negative over the second (lower) factor.

The a priori infinite number of algebraic varieties of general type to serve in such "regularizing" mappings correlates with the infinite number of VEX polytopes usable in encoding the Calabi-Yau models of [5]. Also, this

supports the possibility that the pool of (g)CICYs connects to *all* Calabi-Yau models — including all toric models [6], which resonates with the second part of [36] (and closing paragraph of [19, Ch. D]) that discusses conifold transitions to branched multiple covers.

4. Gauged linear sigma model aspects

Each Cox variable in a toric model is identified 1–1 with a *chiral* superfield of the the gauged linear sigma model (GLSM) [17, 18]. In turn, each toric, i.e., projective space projectivization transformation corresponds to a *twisted-chiral, $U(1; \mathbb{C})$-gauge superfield.* Then, the constant-Jacobian changes of variables such as (2.12a), (2.21), (2.24) and (2.27) correspond to those same superfield redefinitions. In fact, even the non-constant Jacobian changes of variables (3.58) and (3.59) nevertheless turn out to provide supersymmetry-preserving mappings of superfields. This provides a direct "translation" of the toric computations discussed herein into the GLSM framework.

To this end, we focus on *worldsheet* supersymmetry as needed in the usual application of GLSMs, and note that all superfields are formal power-series such as $\boldsymbol{\Phi} = \phi(\xi) + \theta^\alpha \psi_\alpha(\xi) + \theta^2 F(\xi) \dots$ [68–70]. Here, ξ denotes the ordinary (bosonic, commuting) coordinates on the worldsheet, and $\theta^\alpha, \bar{\theta}^{\dot\alpha}$ with $\alpha = 1, 2, \dots, p$ and $\dot\alpha = 1, 2, \dots, q$ denote Grassmann (fermionic, anti-commuting) coordinates of the (p, q)-superspace extension of the worldsheet; routinely, $\theta^2 := \frac{1}{2}(\theta^\alpha \theta^\beta - \theta^\beta \theta^\alpha)$, etc. In this $\theta, \bar{\theta}$-expansion, coefficient functions of even (vs. odd) order, $\phi(\xi), F(\xi), \dots$ (vs. $\psi_\alpha(\xi), \dots$), have the same (vs. opposite) boson/fermion parity as the superfield $\boldsymbol{\Phi}$ itself. Owing to the nilpotence and anticommutativity of $\theta, \bar{\theta}$, all superfields in fact terminate into order-(p, q) polynomials in $\theta, \bar{\theta}$.

Focusing now on $(2, 2)$-supersymmetry and using the customary labels $\alpha, \dot\alpha = -, +$ [71], the particular class of chiral ($\boldsymbol{\Phi}$) and twisted-chiral ($\boldsymbol{\Sigma}$) superfields are specified by the 1st-order superdifferential conditions

$$(4.1) \qquad \bar{D}_\pm \boldsymbol{\Phi} = 0 \qquad \text{and} \qquad \bar{D}_- \boldsymbol{\Sigma} = 0 = D_+ \boldsymbol{\Sigma}.$$

It is immediate that such superfields form a ring under ordinary multiplication and all analytic functions of superfields are also superfields. Moreover, even division by a superfield is well defined as long as division by its leading

("lowest-component") coefficient function, $\phi(\xi)$, is:

$$(4.2) \quad \frac{f(\mathbf{\Phi}_1, \mathbf{\Phi}_2, \dots)}{\mathbf{\Phi}}$$
$$= f(\mathbf{\Phi}_1, \mathbf{\Phi}_2, \dots) \left(\frac{1}{\phi} - (\theta^\pm \psi_\pm + \theta^2 F) \frac{1}{\phi^2} + \theta^2 \psi_- \psi_+ \frac{1}{\phi^3} + \dots \right).$$

Similar $\theta, \bar{\theta}$-expansions are just as well defined for fractional powers[10], such as needed in (3.58) and (3.59). Since chiral superfields in a GLSM are assigned to the Cox variables in the corresponding toric model, the various rational expressions involving chiral superfields are well defined as long as their Cox variable counterparts are. As discussed in §3.2, this is true in all the cases of interest here.

Finally, it remains to ascertain that the Laurent polynomials of chiral superfields as used herein are themselves chiral superfields — as required of the superpotential in the GLSM. In particular, the superpotentials of interest are all of the general form $W(\mathbf{X}) = \mathbf{X}_0\, f(\mathbf{X}_i)$ for $i = 1, 2, \dots$, as we check:

$$(4.3a) \qquad \bar{D}_\pm\big(\mathbf{X}_0\, f(\mathbf{X}_i)\big) = \big(\underbrace{\bar{D}_\pm \mathbf{X}_0}_{=0}\big) f(\mathbf{X}_i) + \mathbf{X}_0 \sum_{i>0} \frac{\partial f}{\partial \mathbf{X}_i} \big(\underbrace{\bar{D}_\pm \mathbf{X}_i}_{=0}\big),$$

$$(4.3b) \qquad\qquad\qquad = 0 \quad \text{precisely if} \quad \big|f(\mathbf{X}_i)\big|, \ \left|\mathbf{X}_0 \frac{\partial f}{\partial \mathbf{X}_i}\right| < \infty,$$

whatever the functional form of $f(\mathbf{X}_i)$. The analogous expansion checks that the so-called twisted superpotential itself remains a twisted chiral superfield.

Now, every *quantum* field can be expanded about a given *vacuum expectation value* (vev), which is also known as the *background field expansion*. The vev of every fermionic component field in every superfield must vanish to preserve Lorentz symmetry, and the vev of every auxiliary field must vanish to preserve supersymmetry [68–70]. It then follows that the vev of any chiral (and also twisted-chiral) superfield reduces to the vev of its lowest component field, $\langle \mathbf{\Phi} \rangle = \langle \phi \rangle$ — which for every "$\theta, \bar{\theta}$-expandable" function $f(\mathbf{X}_i)$ is the *value* of that function of the corresponding Cox variable, $f(X_i)$.

Thus, as long as the vevs of the lowest components of the superfield expressions appearing in the condition of (4.3b) are finite, the superpotential is indeed a chiral superfield. Reduced to the lowest components in the $\theta, \bar{\theta}$-expansion, these expressions include precisely the defining (regular or

---

[10]In fact, logarithms of superfields are quite commonplace in this type of analysis also in the original works [17, 18], and are defined by analogous $\theta, \bar{\theta}$-expansions.

Laurent) section, $f(X_i)$, its gradient components, $\frac{\partial f}{\partial X_i}$, and the Lagrange multiplier-like field, X_0, interpretable as the fibre coordinate of the canonical bundle. As discussed in §3.2, all of these quantities are required to remain finite in all the toric models considered herein, thus verifying that the GLSM superpotential (as well as the twisted superpotential) remain chiral (twisted-chiral) superfields. This then guarantees the various by now standard *non-renormalization* arguments, insuring that the usual computational framework of supersymmetric GLSMs remains valid.

Finally, the various choices of the Mori vectors as discussed in §2 correspond in the GLSM model to specific choices of generators for the $U(1;\mathbb{C}) \times U(1;\mathbb{C})$ gauge symmetry. As discussed in [18] and traced in full detail in [5], the particular choices are distinguished by leaving some of the Cox variables invariant, and so allowing them to acquire nonzero expectation values. The appearance of at least one neutral Cox variable in every such assignment of the $U(1;\mathbb{C}) \times U(1;\mathbb{C})$ charges precisely reflects one of the requirements in the determination of candidate Mori vectors [29]. This then reinterprets the secondary fan as encoding the *phases* of the GLSM and its possible phase transitions [17, 18]. While illustrated in (2.13), (3.27) and (3.28) for the simplest cases[11], this *semiclassical* characteristic of GLSMs is just as computable for all $n \geqslant 2$ and all $m \in \mathbb{Z}$ and all their discrete deformations discussed in §2.5. These *semiclassical* phase diagrams exhibit a detailed m-dependence — unreduced by the Wall isomorphism, $m \simeq m \,(\mathrm{mod}\, n)$, and so indicate an unreduced sequence of novel Calabi-Yau GLSM models.

5. Concluding remarks

Every *configuration* of (generalized) complete intersections in products of projective spaces [19, 72, 73] represents a continuous deformation family of multi-projective complete intersections. We have shown herein that even the very simplest (2.15) among their generalizations [1–4] contain many discretely related toric models. It is tempting and at least logically possible that the pool of gCICYs in fact includes many (if not all) toric constructions as variously sub-generic and even singular models as well as their various smoothings — including the (infinitely many) VEX models with Laurent deformations [5], far exceeding the already immense database [6]. Of course,

---

[11]The Calabi-Yau hypersurfaces in all $n = 2$ cases are of course 2-tori, which exceptionally have a single Kähler class, and for which the shown 2-dimensional secondary fans collapse to a 1-dimensional one.

toric constructions tend to be computationally more approachable, partly because that is where much of the recent computer-aided technology has been developed. We should like to hope that the explicit relations of the kind explored herein will provide for a sinergy between these different approaches, for the benefit of all, including the somewhat more familiar albeit also more involved renditions discussed in §3.5.

The inclusion of singular models such as the Tyurin degenerations (§3.1) also raises an issue, a resolution of which will require further study: Standard methods of cohomology computations on $F_m^{(n)}[c_1]$ for $m \geqslant 3$ are ambiguous: singular spaces admit even different *notions* of cohomology, e.g., [74, 75], with no a priori obvious preference from string theory in these circumstances; see however [76–81]. The reduction $X_m^{(n-1)} = C_m \cup S_m$ with $\operatorname{Sing} X_m^{(n-1)} = C_m \cap S_m$ being very much akin to the so-called "infinite complex structure" limiting form of the Dwork pencil of quintics [58] suggests that Tyurin-degenerate models have an application in string compactifications, the details of which we defer to a future study.

Appendix A. Holomorphic distinctions

Besides the directrix, the Hirzebruch scrolls (2.1) also exhibit both an m-dependent number of exceptional anticanonical sections, $H^0(F_m^{(n)}, \mathcal{K}^*)$, and also an m-dependent number of exceptional local reparametrizations, $H^0(F_m^{(n)}, T)$ — exactly matching the number of local deformations of the complex structure, $H^1(F_m^{(n)}, T)$. We discuss these in turn, and then also the quasi-Fano components in Tyurin degeneration.

A.1. Exceptional anticanonical sections

While there exist exceptional anticanonical sections in $H^0\big(F_{m;0}^{(n)}, \mathcal{K}^*\big)$ for all $n \geqslant 2$ and $m \geqslant 4$ [2], for notational simplicity we illustrate this here with the lowest-n, lowest-m non-trivial example. Consider the simple deformation of Hirzebruch's original hypersurface [12]:

$$(\text{A.1a}) \quad F_{4;\epsilon}^{(2)} = \big\{(x,y) \in \mathbb{P}^2 \times \mathbb{P}^1 : p(x,y) := x_0\,y_0^4 + x_1\,y_1^4 + \epsilon\,x_2\,y_0^2\,y_1^2 = 0\big\},$$

so that $p(x,y) = p_{a(ijkl)} x_a\, y_i y_j y_k y_l$ simplifies:

$$(\text{A.1b}) \qquad p(x,y): \quad p_{0(0000)} = 1, \quad p_{1(1111)} = 1, \quad p_{2(0011)} = \epsilon$$

The anticanonical sections are determined by the Koszul resolution of $\mathcal{K}^* = \mathcal{O}\big(-\tfrac{1}{2}\big)\big|_{F_{4;\epsilon}^{(2)}}$, where we stack the cohomology groups underneath the corresponding bundles and write the explicit tensor coefficients [19]:

(A.2)

$$
\begin{array}{ccc}
\mathcal{O}\big(-\tfrac{1}{6}\big) & \xrightarrow{\wedge p} & \mathcal{O}\big(-\tfrac{2}{2}\big) \xrightarrow{\rho_{\mathfrak{F}}} \mathcal{K}^* = \mathcal{O}\big(-\tfrac{1}{2}\big)\big|_{F_{4;\epsilon}^{(2)}} \\
\hline
0 & 0 & H^0(F_{4;\epsilon}^{(2)}, \mathcal{K}^*)_{\scriptscriptstyle\triangleleft} \\
\hookrightarrow\{\varphi_a^{i(jk_1\cdots k_4)}\} & \xrightarrow{p} \{\varepsilon^{ij}\phi_{(ab)}\} \to & H^1(F_{4;\epsilon}^{(2)}, \mathcal{K}^*) \\
0 & 0 & H^2(F_{4;\epsilon}^{(2)}, \mathcal{K}^*)=0 \\
0 & 0 & -
\end{array}
$$

$$H^0(F_{2;\epsilon}^{(2)}, \mathcal{K}^*) \sim \ker\big[\underbrace{\{\varphi_a^{i(jk_1\cdots k_4)}\}}_{\dim = 15} \xrightarrow{p} \underbrace{\{\varepsilon^{ij}\phi_{(ab)}\}}_{\dim = 6}\big],$$

$$H^1(F_{2;\epsilon}^{(2)}, \mathcal{K}^*) \sim \operatorname{coker}\big[\underbrace{\{\varphi_a^{i(jk_1\cdots k_4)}\}}_{} \xrightarrow{p} \underbrace{\{\varepsilon^{ij}\phi_{(ab)}\}}_{}\big],$$

where $\varphi^{i(jk_1\cdots k_4)} \approx \varepsilon^{i(j}\varphi^{k_1\cdots k_4)}$ is totally symmetric in $(jk_1\cdots k_4)$, but vanishes on total symmetrization of all indices, $\varphi^{(i(jk_1\cdots k_4))} = 0$.

With the choice (A.1), the kernel of the p-mapping in (A.2), $\varphi_{(a}^{i(jk_1\cdots k_4)}\, p_{b)(k_1\cdots k_4)} \mapsto \varepsilon^{ij}\phi_{(ab)}$, is spanned by the non-zero solutions of the system

$$(\text{A.3}) \quad \begin{aligned} &\big\{\varphi_{(a}^{i(jk_1\cdots k_4)}\, p_{b)(k_1\cdots k_4)} = 0\big\} \\ &\quad \varphi^{i(jk_1\cdots k_4)} \approx \varepsilon^{i(j}\varphi^{k_1\cdots k_4)} \end{aligned}$$

$$= \left\{ \begin{array}{lll} \varphi_1^{1111} = 0, & \varphi_1^{0000} + \varphi_0^{1111} = 0, & \varphi_0^{0000} = 0 \\ 6\epsilon\,\varphi_1^{0011} + \varphi_2^{1111} = 0, & 6\epsilon\,\varphi_0^{0011} + \varphi_2^{0000} = 0, & \epsilon\,\varphi_2^{0011} = 0 \end{array} \right\}$$

When $\epsilon \neq 0$, all six equations (A.3) constrain, and $H^0(F_{2;\epsilon}^{(2)}, \mathcal{K}^*)$ is spanned by the $\dim \ker(p) = 15 - 6 = 9$ coefficients:

$$(\text{A.4}) \qquad \varphi_1^{0000}, \quad \varphi_0^{0011}, \quad \varphi_1^{0011}, \quad \text{and} \quad \varphi_a^{0001}, \quad \varphi_a^{0111} \quad \text{for} \quad a = 0, 1, 2.$$

However, on Hirzebruch's original hypersurface $\epsilon = 0$, the very last of the six equations (A.3) is vacuous, and φ_2^{0011} is additionally left unconstrained.

This leaves now a total of ten free coefficients to parametrize anticanonical sections via the general formula [2],

$$(A.5) \qquad q(x,y) = \varphi_{(a}^{i(j_1 \cdots j_5)} \, p_{b)(i\,j_3 \cdots j_5)} \, \frac{x^a \, x^b}{h^{(j_1 j_2)}(y)},$$

and the exceptional contribution parametrized by φ_2^{0011} is no different. This not only confirms the counting based on $F_4^{(2)} := \mathbb{P}(\mathcal{O} \oplus \mathcal{O}(4))$ provided in [2], but explicitly constructs this exceptional anticanonical section. The by now standard argument [1, 2] as well as the general scheme-theoretic framework [3, 4] verify that all so-constructed exceptional anticanonical sections are also holomorphic on $F_4^{(2)}$.

In turn, the cokernel of the p-mapping in (A.2), $\{\varepsilon^{ij}\phi_{(ab)}$ $(\mathrm{mod}\ \varepsilon^{i(j}\varphi_{(a}^{k_1 \cdots k_4)} \, p_{b)(k_1 \cdots k_4)})\}$ has all $\binom{2+2}{2} = 6$ parameters $\phi_{(ab)}$ gauged away if $\epsilon \neq 0$, leaving nothing to parametrize $H^1(F_{2;\epsilon}^{(2)}, \mathcal{K}^*) = 0$. In particular, $\varepsilon^{ij}\phi_{(22)}$ is gauged away by $\varepsilon^{i(j}\varphi_{(2}^{k_1 \cdots k_4)} \, p_{2)(k_1 \cdots k_4)} = \epsilon \, \varepsilon^{i(j}\varphi_2^{0011)}$, since $p_{2(k_1 \cdots k_2)} = p_{2(0011)} = \epsilon$. However, on Hirzebruch's original hypersurface when $\epsilon = 0$, the contribution $\phi_{(22)} \mapsto H^1(F_{2;\epsilon}^{(2)}, \mathcal{K}^*)$ is not gauged away, leaving $\dim H^1(F_{2;\epsilon}^{(2)}, \mathcal{K}^*) = 1$.

These computations generalize straightforwardly to all $m \geqslant 4$ and $n \geqslant 2$, and verify the result [2] for these sub-generic hypersurfaces:

$$(A.6a) \qquad \dim H^0(F_{m;\epsilon}^{(n)}, \mathcal{K}^*) = 3\binom{2n-1}{n} + \hat{\delta}_{m;\epsilon}^{(n)}$$
$$\text{and} \quad \dim H^1(F_{m;\epsilon}^{(n)}, \mathcal{K}^*) = \hat{\delta}_{m;\epsilon}^{(n)},$$

where the number of exceptional contributions is

$$(A.6b) \qquad \hat{\delta}_{m;0}^{(n)} = \vartheta_3^m \binom{2n-2}{2}(m-3),$$
$$\text{for} \quad F_{m,0}^{(n)} = \{x_0 \, y_0^{\,m} + x_1 \, y_1^{\,m} = 0\} \in \left[\begin{smallmatrix}\mathbb{P}^n \\ \mathbb{P}^1\end{smallmatrix} \middle\| \begin{smallmatrix}1 \\ m\end{smallmatrix}\right],$$
$$(A.6c) \qquad \hat{\delta}_{m;\epsilon \neq 0}^{(n)} < \hat{\delta}_{m;0}^{(n)}; \quad \text{for generic cases,}\ \hat{\delta}_{m;\epsilon \neq 0}^{(n)} = 0.$$

Between Hirzebruch's central, maximally *non-generic* hypersurface (2.1) and the maximally generic deformations (2.2), there may well exist intermediately sub-generic hypersurfaces for which the number of exceptional anticanonical sections is also nonzero, depends on the ϵ's, but does not reach the maximal value $\vartheta_3^m \binom{2n-2}{2}(m-3)$.

This "jumping" (A.6a) in the dimensions of $H^*(F_{m;\epsilon}^{(n)}, \mathcal{K}^*)$ depending on the concrete choice of the defining equation (2.1)–(2.2) illustrates the fact that a deformation family of even simple hypersurfaces such as $\left[\begin{smallmatrix}\mathbb{P}^n \\ \mathbb{P}^1\end{smallmatrix} \middle\| \begin{smallmatrix}1 \\ m\end{smallmatrix}\right]$ easily contain *discretely different* complex manifolds.

A.2. Exceptional local reparametrizations

Another consequence of this complex structure subtlety is the existence of the exceptional local reparametrizations of $F_m^{(n)}$, parametrized by $H^0(F_m^{(n)}, T)$. As a holomorphic cohomology computation, this again showcases the subtle dependence on the complex structures.

Suffices it again to consider but the simplest, $n=2$ cases, and compute the cohomology groups $H^*(F_{m;\epsilon}^{(2)}, T)$ for deformed hypersurfaces such as (2.2) and (A.1), parametrizing the complex structures of those hypersurfaces $F_{m;\epsilon}^{(2)} \in \left[\begin{smallmatrix}\mathbb{P}^2 \\ \mathbb{P}^1\end{smallmatrix}\middle\|\begin{smallmatrix}1 \\ m\end{smallmatrix}\right]$. To this end, we use the adjunction formula combined with the Koszul resolution of the restriction to $F_{m;\epsilon}^{(2)}$ of requisite bundles:

(A.7)
$$
\begin{array}{ccccccc}
T_A \otimes \mathcal{O}_A\left(\begin{smallmatrix}-1\\-m\end{smallmatrix}\right) & & \mathcal{O}_A & & & & \\
\uparrow p & & \uparrow p & & & & \\
T_A & & \mathcal{O}_A\left(\begin{smallmatrix}1\\m\end{smallmatrix}\right) & \text{i.e.} & & & \\
\downarrow \rho & & \downarrow \rho & & & & \\
T_{F_{m;\epsilon}^{(2)}} \hookrightarrow & T_A|_{F_{m;\epsilon}^{(2)}} & \twoheadrightarrow \mathcal{O}_{F_{m;\epsilon}^{(2)}}\left(\begin{smallmatrix}1\\m\end{smallmatrix}\right) & & & &
\end{array}
$$

$$
\begin{array}{ccc}
\left(\begin{smallmatrix}0\\m\end{smallmatrix}\middle|\begin{smallmatrix}0\ 1\\0\end{smallmatrix}\right) \oplus \left(\begin{smallmatrix}1\\m-1\end{smallmatrix}\middle|\begin{smallmatrix}0\ 0\\1\end{smallmatrix}\right) & & \left(\begin{smallmatrix}0\\0\end{smallmatrix}\middle|\begin{smallmatrix}0\ 0\\0\end{smallmatrix}\right) \\
\uparrow p & & \uparrow p \\
\left(\begin{smallmatrix}-1\\0\end{smallmatrix}\middle|\begin{smallmatrix}0\ 1\\0\end{smallmatrix}\right) \oplus \left(\begin{smallmatrix}0\\-1\end{smallmatrix}\middle|\begin{smallmatrix}0\ 0\\1\end{smallmatrix}\right) & & \left(\begin{smallmatrix}-1\\-m\end{smallmatrix}\middle|\begin{smallmatrix}0\ 0\\0\end{smallmatrix}\right) \\
\downarrow \rho & & \downarrow \rho \\
T_{F_{m;\epsilon}^{(2)}} \hookrightarrow \quad T_A|_{F_{m;\epsilon}^{(2)}} & & \twoheadrightarrow \mathcal{O}_{F_{m;\epsilon}^{(2)}}\left(\begin{smallmatrix}1\\m\end{smallmatrix}\right)
\end{array}
$$

where "$(a|b_1 b_2)$" encodes bundles on $\mathbb{P}^2 = \frac{U(3)}{U(1)\times U(2)}$ in terms of $U(1)\times U(2)$-representations: a is the $U(1)$ charge, and $(b_1 b_2)$ encodes the $U(2)$-representation by means of the Young tableau with b_r boxes in the rth row. Analogously, $\mathbb{P}^1 = \frac{U(2)}{U(1)\times U(1)}$, and "$\left(\begin{smallmatrix}a\\c\end{smallmatrix}\middle|\begin{smallmatrix}b_1\ b_2\\d\end{smallmatrix}\right)$" encodes bundles on $\mathbb{P}^2 \times \mathbb{P}^1$ [19, 82, 83].

The central column in (A.7) produces

(A.8)

	$\left(\begin{smallmatrix}0\\m\end{smallmatrix}\middle|\begin{smallmatrix}0\ 1\\0\end{smallmatrix}\right) \oplus \left(\begin{smallmatrix}1\\m-1\end{smallmatrix}\middle|\begin{smallmatrix}0\ 0\\1\end{smallmatrix}\right)$	$\left(\begin{smallmatrix}-1\\0\end{smallmatrix}\middle|\begin{smallmatrix}0\ 1\\0\end{smallmatrix}\right) \oplus \left(\begin{smallmatrix}0\\-1\end{smallmatrix}\middle|\begin{smallmatrix}0\ 0\\1\end{smallmatrix}\right)$	$T_A|_{F_{m;\epsilon}^{(2)}}$
0.	$\vartheta_m^0\{\varphi^a\}_1^3 \xrightarrow{\ p\ } \{\lambda_b{}^a\}_1^8 \oplus \{\kappa_j{}^i\}_3^1$		$H^0(F_{m;\epsilon}^{(2)}, T_A)$
1.	$\vartheta_2^m\{\varphi^{i(j_2\cdots i_m)a}\}_{m-1}^3$	0	0
$\vdots$	$\vdots$	$\vdots$	$\vdots$

(A.9) $\quad H^0(F_{m;\epsilon}^{(2)}, T_A) \sim \{\lambda_b{}^a/(\vartheta_m^0 \varphi^a p_b)\} \oplus \{\kappa_j{}^i\} \circledast \{\vartheta_2^m \varkappa_j{}^i\}$

where "$\overline{\mathbf{1\ 0\ 0}}$" indicates no cohomology, $\vartheta_a^b := \{1 \text{ if } a \leqslant b, \ 0 \text{ otherwise}\}$, the "directed sum" $A \circledast B = C$ denotes the *extension of B by A*, i.e., abbreviates the exact sequence $A \hookrightarrow C \twoheadrightarrow B$, and where

(A.10) $\qquad y^j \varkappa_j{}^i \dfrac{\partial}{\partial y^i}, \qquad \text{with} \quad \varkappa_j{}^i := \varphi^{i(k_2\cdots k_m)a} \, p_{a(jk_2\cdots k_m)},$

is the minimal form of this contribution to reparametrizations, constructed by maximally contracting the tensor coefficients[12]. This gives $\dim H^0(F^{(2)}_{m;\epsilon}, T_A) = (8 - \vartheta^0_m 3) + 3 + \vartheta^m_2 3(m-1) = 3m+8$.

The right-hand column in (A.7) produces

$$
\begin{array}{c|ccc}
 & \left(\begin{smallmatrix}0 \\ 0\end{smallmatrix}\middle|\begin{smallmatrix}0 & 0\end{smallmatrix}\right) & \left(\begin{smallmatrix}-1 \\ -m\end{smallmatrix}\middle|\begin{smallmatrix}0 & 0\end{smallmatrix}\right) & \mathcal{O}(\begin{smallmatrix}1 \\ m\end{smallmatrix})|_{F^{(2)}_{m;\epsilon}} \\
\hline
0. & \{\vartheta\}^1_1 \xrightarrow{p} \{\phi_{a(i_1,\cdots,i_m)}\}^3_{m+1} & & H^0\big(F^{(2)}_{m;\epsilon}, \mathcal{O}(\begin{smallmatrix}1 \\ m\end{smallmatrix})\big) \\
1. & 0 & 0 & 0 \\
\vdots & \vdots & \vdots & \vdots
\end{array}
$$

(A.11)

(A.12) $\qquad H^0\big(F^{(2)}_{m;\epsilon}, \mathcal{O}(\begin{smallmatrix}1 \\ m\end{smallmatrix})\big) \sim \{\phi_{a(i_1,\cdots,i_m)}/\vartheta\, p_{a(i_1,\cdots,i_m)}\}_{3m+2}.$

Finally, the long exact sequence from the bottom-row short exact sequence in (A.7) reduces to:

(A.13) $\qquad H^0(F^{(2)}_{m;\epsilon}, T) \hookrightarrow \underbrace{\{\lambda_b{}^a/(\vartheta^0_m \varphi^a p_b)\} \oplus \{\kappa_j{}^i\} \circledS \{\vartheta^m_2 \varkappa_j{}^i\}}_{3m+8}$

$$\xrightarrow{\mathrm{d}p} \underbrace{\{\phi_{a(i_1,\cdots,i_m)}/\vartheta\, p_{a(i_1,\cdots,i_m)}\}}_{3m+2} \to H^1(F^{(2)}_{m;\epsilon}, T).$$

This leaves $\dim H^0(F^{(2)}_{m;\epsilon}, T) = 6 + \Delta_m$ reparametrizations and $\dim H^1(F^{(2)}_{m;\epsilon}, T) = \Delta_m$ (Kodaira-Spencer) deformations of the complex structure. The quantity $\Delta_m = \dim(\mathrm{coker}(\mathrm{d}p))$ measures the corank of the $\mathrm{d}p$-mapping, i.e., $\Delta_m = 0$ if $\mathrm{d}p$ is of maximal rank.

As the simplest concrete and non-trivial example, consider the $m=2=n$ family

(A.14)
$$F^{(2)}_{2;\epsilon} := \{p_{\vec{\epsilon}}(x,y)=0\} \in \begin{bmatrix} \mathbb{P}^2 & \Big\| & 1 \\ \mathbb{P}^1 & & 2 \end{bmatrix},$$

$$p_{\vec{\epsilon}}(x,y) := x_0\, y_0^2 + x_1\, y_1^2 + \epsilon\, x_2\, y_0 y_1$$

for which we have:
(A.15)
$$H^0\big(F^{(2)}_{m;\epsilon}, T\big) \hookrightarrow \{\lambda_b{}^a\} \oplus \{\kappa_j{}^i\} \circledS \{\varkappa_j{}^i\} \xrightarrow{\mathrm{d}p} \{\phi_{a(ij)}/\varphi\, p_{a(ij)}\} \twoheadrightarrow H^1(F^{(2)}_{m;\epsilon}, T),$$

$$\big(\lambda_a{}^b\, p_{b(ij)} + p_{a\,k(i}\,\kappa_{j)}{}^k + p_{a\,k(i}\,\varkappa_{j)}{}^k\big) =: \widehat{\phi}_{a(ij)}.$$

---

[12]Iteratively "un-contracting" this expression, $\varphi^{\cdots i)a}p_{\cdots j)}\,\delta_i{}^j \to \varphi^{\cdots i)a}p_{\cdots j)}\frac{y^j}{y^i} \to$ etc., generalizes the representatives and enables a detailed and complete match with the direct Czech cohomology computations à la Ref. [4].

With (A.14) and so $p_{0(00)} = 1 = p_{1(11)}$ and $p_{2(01)} = \epsilon$, the definition (A.10) of $\varkappa_j^k$ specifies

$$(A.16) \qquad \varkappa_0^1 = -\varphi^0, \quad \varkappa_1^0 = \varphi^1, \quad \text{and} \quad \varkappa_0^0 = \epsilon\,\varphi^2 = -\varkappa_1^1.$$

$H^0(F_{m;\epsilon}^{(2)}, T) = \ker(\mathrm{d}p)$ is spanned by the variables $\{\lambda_b^a, \kappa_j^i, \varkappa_j^i\}$ omitted in the assignment (A.15) in the target spanned by elements of the equivalence class $[\phi_{a(ij)} \simeq \phi_{a(ij)} + \varphi\, p_{a(ij)}]$:

$$(A.17) \quad \lambda_a^b\, p_{b(ij)} + p_{a\,k(i}\,\kappa_{j)}{}^k + p_{a\,k(i}\,\varkappa_{j)}{}^k \quad \mapsto \quad [\phi_{a(ij)} \simeq \phi_{a(ij)} + \varphi\, p_{a(ij)}].$$

While $\phi_{a(ij)}$ has $\binom{1+2}{2}\binom{2+1}{1} = 9$ components, the mod $p_{\vec{\epsilon}}(x,y)$-equivalence class on the right-hand side has $9-1=8$, so that (A.17) encodes only 8 equations, not 9. With the choice (A.14),

$$(A.18) \quad [\phi_{a(ij)} \simeq \phi_{a(ij)} + \varphi\, p_{a(ij)}] \sim$$
$$\left\{ \begin{array}{l} \phi_{0(01)}, \quad \phi_{0(11)}, \quad \phi_{1(00)}, \quad \phi_{1(01)}, \quad \phi_{2(00)}, \quad \phi_{2(11)}, \\ \phi_{0(00)} \simeq \phi_{0(00)} + \varphi, \quad \phi_{1(11)} \simeq \phi_{1(11)} + \varphi, \quad \phi_{2(01)} \simeq \phi_{2(01)} + \epsilon\,\varphi \end{array} \right\}.$$

The $\varphi = -\phi_{0(00)}$ "gauge" renders the $\widehat{\phi}_{0(00)} = 0$ equation vacuous, and replaces

$$(A.19) \qquad \widehat{\phi}_{1(11)} \rightarrow (\widehat{\phi}_{1(11)} - \widehat{\phi}_{0(00)}) \quad \text{and} \quad \widehat{\phi}_{2(01)} \rightarrow (\widehat{\phi}_{2(01)} - \epsilon\,\widehat{\phi}_{0(00)}),$$

turning the system of assignments (A.15) into:

(A.20)

a	$(ij)=(00)$	$(ij)=(01)$	$(ij)=(11)$
0	——	$2\epsilon\,\lambda_0^2 + (\kappa_1^0 + \varkappa_1^0) \mapsto 2\phi_{0(01)}$	$\lambda_0^1 \mapsto \phi_{0(11)}$
1	$\lambda_1^0 \mapsto \phi_{1(00)}$	$2\epsilon\,\lambda_1^2 + (\kappa_0^1 + \varkappa_0^1) \mapsto 2\phi_{1(01)}$	$\lambda_0^0 - \lambda_1^1 + 2(\kappa_0^0 + \varkappa_0^0) \mapsto \phi_{1(11)}$
2	$\lambda_2^0 + \epsilon(\kappa_0^1 + \varkappa_0^1) \mapsto \phi_{2(00)}$	$-\epsilon\big(2\lambda_0^0 + \lambda_1^1 + (\kappa_0^0 + \varkappa_0^0)\big) \mapsto 2\phi_{2(01)}$	$\lambda_2^1 + \epsilon(\kappa_1^0 + \varkappa_1^0) \mapsto \phi_{2(11)}$

For $\epsilon \neq 0$, the system is solved by assigning, e.g.:

$$(A.21a) \qquad \varkappa_0^0 \mapsto \left(\tfrac{1}{2\epsilon}\phi_{2(01)} + \lambda_1^1\right) - \tfrac{1}{2}\phi_{1(11)} - \kappa_0^0, \quad \lambda_0^0 \mapsto -\left(\tfrac{1}{\epsilon}\phi_{2(01)} - \lambda_1^1\right),$$
$$\lambda_0^1 \mapsto \phi_{0(11)}, \quad \lambda_1^0 \mapsto \phi_{1(00)},$$

$$(A.21b) \qquad \varkappa_0^1 \mapsto 2\phi_{1(01)} - \kappa_0^1 - 2\epsilon\lambda_1^2, \quad \lambda_2^0 \mapsto \phi_{2(00)} + 2\epsilon^2\lambda_1^2 - 2\epsilon\phi_{1(01)},$$

$$(A.21c) \qquad \varkappa_1^0 \mapsto 2\phi_{0(01)} - \kappa_1^0 - 2\epsilon\lambda_0^2,$$
$$\lambda_2^1 \mapsto \phi_{2(11)} - \epsilon(2\phi_{0(01)} + \tfrac{1}{2}\phi_{1(11)}) + \tfrac{1}{2}\epsilon(\lambda_0^0 + \lambda_1^1) + 2\epsilon^2\lambda_0^2,$$

which leaves six linearly independent local reparametrization generator representatives

$$(A.22) \quad H^0(F^{(2)}_{m;\epsilon}, T) \sim$$
$$\left\{ x^1\lambda_1{}^1 \frac{\partial}{\partial x^1},\ x^0\lambda_0{}^2 \frac{\partial}{\partial x^2},\ x^1\lambda_1{}^2 \frac{\partial}{\partial x^2},\ y^0\kappa_0{}^0 \frac{\partial}{\partial y^0},\ y^1\kappa_1{}^0 \frac{\partial}{\partial y^0},\ y^0\kappa_0{}^1 \frac{\partial}{\partial y^1} \right\}.$$

At $\epsilon \to 0$, the (middle-column, bottom-row) $\phi_{2(01)}$-assignment becomes vacuous, reducing the system from eight equations to seven, increasing $\dim H^0(F^{(2)}_{m;\epsilon}, T) = 6 \to 7$ and $\dim H^1(F^{(2)}_{m;\epsilon}, T) = 0 \to 1$. The $\epsilon \to 0$ limit of the system (A.20) is solved by the straightforward $\epsilon \to 0$ limit of the replacements (A.21) except that now

$$(A.23) \qquad \epsilon \to 0: \qquad \varkappa_0{}^0 \to -\tfrac{1}{2}\phi_{1(11)} + \tfrac{1}{2}(\lambda_1{}^1 - \lambda_0{}^0) - \kappa_0{}^0, \qquad \lambda_0{}^0 \text{ free},$$

adding $x^0\lambda_0{}^0 \frac{\partial}{\partial x^0}$ to $H^0(F^{(2)}_{m;0}, T)$, and leaving $\phi_{2(01)} \in H^1(F^{(2)}_{m;0}, T)$ for the central, $\epsilon = 0$ member of the deformation family, the original Hirzebruch surface.

This explicit (if tedious) construction generalizes to all $m, n \geqslant 2$, and produces the above-quoted results (2.7), and is in full agreement with the SAGE result for the automorphism group of the toric realization of $F^{(n)}_m$. As with $H^*(F^{(n)}_m, \mathcal{K}^*)$, the deformation family (2.2) may well contain sub-generic hypersurfaces for which the number of exceptional reparametrizations is also nonzero, depends on the ϵ's, but does not reach the maximal value $\vartheta^m_1 (n-1)(m-1)$.

A.3. Quasi-Fano components

The cohomology of the components $\big(S_m = \mathfrak{s}^{-1}(0)\big)$, $\big(C_m = \mathfrak{c}^{-1}(0)\big) \subset F^{(n)}_m$ is readily computed, as we show here using the bi-projective embedding (2.1). The results,

$$(A.24) \quad \dim H^r(S_m, \mathcal{O}) = \delta_{r,0} = \dim H^r(C_m, \mathcal{O}), \quad \chi(\mathcal{O}_{S_m}) = 1 = \chi(\mathcal{O}_{C_m})$$

and the fact that $S_m \cap C_m = {}^\sharp X^{(n-2)}_m$ is a smooth Calabi-Yau space for generic choices of $\mathfrak{c}(x, y)$ satisfies the definition [35, Def. 2.2] of a *quasi-Fano* space.

The directrix. Consider first the hallmark directrix hypersurface $S_m \subset F^{(n)}_m$. Its structure sheaf cohomology is computed from the network

of Koszul resolutions:

(A.25)
$$
\begin{array}{ccc}
\mathcal{O}_A\!\left(\begin{smallmatrix}-2\\0\end{smallmatrix}\right) & \overset{\mathfrak{s}}{\hookrightarrow} & \mathcal{O}_A\!\left(\begin{smallmatrix}-1\\-m\end{smallmatrix}\right)\\
{\scriptstyle\int p_0}\uparrow & & {\scriptstyle\int p_0}\uparrow\\
\mathcal{O}_A\!\left(\begin{smallmatrix}-1\\m\end{smallmatrix}\right) & \overset{\mathfrak{s}}{\hookrightarrow} & \mathcal{O}_A\\
\downarrow & & \downarrow\\
\mathcal{O}_{F_m^{(n)}}\!\left(\begin{smallmatrix}-1\\m\end{smallmatrix}\right) & \overset{\mathfrak{s}}{\longrightarrow} & \mathcal{O}_{F_m^{(n)}} & \twoheadrightarrow & \mathcal{O}_{S_m}
\end{array}
$$

where the mapping induced from multiplication by $\mathfrak{s}(x,y)$ becomes regular on $F_m^{(n)}$ (in the bottom row), while elsewhere on A it involves multiplication by the equivalence class of Laurent polynomials (2.11). The vertical sequences are however induced from multiplication by the polynomial $p_0(x,y)$, which is regular everywhere on A. We compute the associated cohomology from those first, using again the Young tableau notation as above [19]:

(A.26)
$$
\begin{array}{c|ccc}
& \left(\begin{smallmatrix}2&0&\cdots&0\\0&0\end{smallmatrix}\right) \overset{p_0}{\longrightarrow} \left(\begin{smallmatrix}1&0&\cdots&0\\-m&0\end{smallmatrix}\right) \twoheadrightarrow \mathcal{O}_{F_m^{(n)}}\!\left(\begin{smallmatrix}-1\\m\end{smallmatrix}\right)\\
\hline
0. & 0 & 0 & H^0=0\\
1. & 0 & 0 & H^1=0\\
\vdots & \vdots & \vdots & \vdots
\end{array}
$$

$$
\text{and}\quad
\begin{array}{c|cccc}
& & \left(\begin{smallmatrix}1&0&\cdots&0\\m&0\end{smallmatrix}\right) \overset{p_0}{\longrightarrow} \left(\begin{smallmatrix}0&0&\cdots&0\\0&0\end{smallmatrix}\right) \twoheadrightarrow \mathcal{O}_{F_m^{(n)}}\\
\hline
0. & 0 & \left(\begin{smallmatrix}0&0&\cdots&0\\0&0\end{smallmatrix}\right) \approx H^0\\
1. & 0 & 0 & H^1=0\\
\vdots & \vdots & \vdots & \vdots
\end{array}
$$

Combining these results for the bottom, horizontal sequence in (A.25) yields

(A.27)
$$
\begin{array}{c|cccc}
& \mathcal{O}_{F_m^{(n)}}\!\left(\begin{smallmatrix}-1\\m\end{smallmatrix}\right) \overset{\mathfrak{s}}{\hookrightarrow} \mathcal{O}_{F_m^{(n)}} \twoheadrightarrow \mathcal{O}_{S_m}\\
\hline
0. & 0 & \left(\begin{smallmatrix}0&0&\cdots&0\\0&0\end{smallmatrix}\right) \approx H^0 \approx \mathbb{C}\\
1. & 0 & 0 & H^1=0\\
\vdots & \vdots & \vdots & \vdots
\end{array}
\qquad \text{so}\quad \chi(\mathcal{O}_{S_m})=1.
$$

The complemetrix. The analogous computation for the complementrix, $(C_m \subset F_m^{(n)}) \in \left[\begin{smallmatrix}\mathbb{P}^n\\\mathbb{P}^1\end{smallmatrix}\middle\|\begin{smallmatrix}1&n-1\\m&2\end{smallmatrix}\right]$, is:

(A.28)
$$
\begin{array}{ccccc}
\mathcal{O}_A\!\left(\begin{smallmatrix}-n\\-2-m\end{smallmatrix}\right) & \overset{\mathfrak{c}}{\hookrightarrow} & \mathcal{O}_A\!\left(\begin{smallmatrix}-1\\-m\end{smallmatrix}\right) & \twoheadrightarrow & \mathcal{O}_{C'_m}\!\left(\begin{smallmatrix}-1\\-m\end{smallmatrix}\right)\\
{\scriptstyle\int p_0}\uparrow & & {\scriptstyle\int p_0}\uparrow & & {\scriptstyle\int p_0}\uparrow\\
\mathcal{O}_A\!\left(\begin{smallmatrix}1-n\\-2\end{smallmatrix}\right) & \overset{\mathfrak{c}}{\hookrightarrow} & \mathcal{O}_A & \twoheadrightarrow & \mathcal{O}_{C'_m}\\
\downarrow & & \downarrow & & \downarrow\\
\mathcal{O}_{F_m^{(n)}}\!\left(\begin{smallmatrix}1-n\\-2\end{smallmatrix}\right) & \overset{\mathfrak{c}}{\hookrightarrow} & \mathcal{O}_{F_m^{(n)}} & \twoheadrightarrow & \mathcal{O}_{C_m}
\end{array}
\qquad \text{where}\quad
\begin{cases}
C'_m \in \left[\begin{smallmatrix}\mathbb{P}^n\\\mathbb{P}^1\end{smallmatrix}\middle\|\begin{smallmatrix}n-1\\2\end{smallmatrix}\right],\\
C'_m := \{\mathfrak{c}(x,y)=0\} \subset A.
\end{cases}
$$

Since both $p_0(x,y)$ and $\mathfrak{c}(x,y)$ are regular polynomials on $A = \mathbb{P}^n \times \mathbb{P}^1$, both the horizontal and the vertical mappings are well defined over all of A, and we short-cut the cohomology computation using the spectral sequence [19]:

(A.29)

$$
\left(\begin{smallmatrix} n & | & 0 \cdots & 0 \\ 2+m & | & 0 \end{smallmatrix}\right) \overset{\mathfrak{c}}{\underset{p_0}{\rightrightarrows}} \left(\begin{smallmatrix} 1 & | & 0 \cdots & 0 \\ m & | & 0 \\ n & | & 0 \cdots & 0 \\ 2 & | & 0 \end{smallmatrix}\right) \overset{p_0}{\underset{\mathfrak{c}}{\rightrightarrows}} \left(\begin{smallmatrix} 0 & | & 0 \cdots & 0 \\ 0 & | & 0 \end{smallmatrix}\right) \twoheadrightarrow \mathcal{O}_{C_m}
$$

0.	0	0	$\left(\begin{smallmatrix}0 & 0 \cdots & 0 \\ 0 & 0\end{smallmatrix}\right) \approx H^0 \approx \mathbb{C}$	so $\chi(\mathcal{O}_{C_m}) = 1.$
1.	0	0	0	$H^1 = 0$
⋮	⋮	⋮	⋮	⋮

References

[1] L. B. Anderson, F. Apruzzi, X. Gao, J. Gray, and S.-J. Lee, "A new construction of Calabi-Yau manifolds: Generalized CICYs," *Nucl. Phys.* **B906** (2016) 441–496.

[2] P. Berglund and T. Hübsch, "On Calabi-Yau generalized complete intersections from Hirzebruch varieties and novel K3-fibrations," *Adv. Theor. Math. Phys.* **22** no. 2, (2018) 261–303.

[3] Q. Jia and H. Lin, "Calabi-Yau generalized complete intersections and aspects of cohomology of sheaves," *J. Math. Phys.* **61** no. 5, (2020) 052301.

[4] A. Garbagnati and B. van Geemen, "A remark on generalized complete intersections," *Nucl. Phys.* **B925** (2017) 135–143.

[5] P. Berglund and T. Hübsch, "A generalized construction of Calabi-Yau models and mirror symmetry," *SciPost* **4** no. 2, (2018) 009 (1–30).

[6] M. Kreuzer and H. Skarke, "Complete classification of reflexive polyhedra in four dimensions," *Adv. Theor. Math. Phys.* **4** no. 6, (2002) 1209–1230.

[7] P. Berglund and T. Hübsch, "A generalized construction of mirror manifolds," *Nucl. Phys.* **B393** no. 1-2, (1993) 377–391.

[8] P. Berglund and M. Henningson, "Landau-Ginzburg orbifolds, mirror symmetry and the elliptic genus," *Nucl. Phys.* **B433** (1995) 311–332.

[9] M. Krawitz, *FJRW rings and Landau-Ginzburg Mirror Symmetry.* PhD thesis, University of Michigan, Ann Arbor, MI, 2010.

[10] V. V. Batyrev, "Dual polyhedra and mirror symmetry for Calabi-Yau hypersurfaces in toric varieties," *J. Alg. Geom.* **3** no. 3, (1994) 493–535.

[11] D. Favero and T. L. Kelly, "Derived categories of BHK mirrors," *Adv. Math.* **352** (2019) 943–980.

[12] F. Hirzebruch, "Über eine Klasse von einfach-zusammenhängenden komplexen Mannigfaltigkeiten," *Math. Ann.* **124** (1951) 77–86.

[13] W. Fulton, *Introduction to Toric Varieties*. Annals of Mathematics Studies. Princeton University Press, 1993.

[14] G. Ewald, *Combinatorial Convexity and Algebraic Geometry*. Springer Verlag, 1996.

[15] D. A. Cox, J. B. Little, and H. K. Schenck, *Toric Varieties*. Graduate Studies in Mathematics. American Mathematical Society, 2011.

[16] P. Griffiths and J. Harris, *Principles of algebraic geometry*. Wiley Classics Library. John Wiley & Sons Inc., New York, 1978.

[17] E. Witten, "Phases of $N = 2$ theories in two-dimensions," *Nucl. Phys.* **B403** (1993) 159–222.

[18] D. R. Morrison and M. R. Plesser, "Summing the instantons: Quantum cohomology and mirror symmetry in toric varieties," *Nucl. Phys.* **B440** (1995) 279–354.

[19] T. Hübsch, *Calabi-Yau Manifolds: a Bestiary for Physicists*. World Scientific Publishing Co. Inc., River Edge, NJ, 2nd ed., 1994.

[20] C. T. C. Wall, "Classifications problems in differential topology V: On certain 6-manifolds," *Invent. Math* **1** (1966) 355–374.

[21] M. Kreck and D. Crowley, "Hirzebruch surfaces," *Bulletin of the Manifold Atlas* no. 19-22, (2011) .

[22] P. S. Green and T. Hübsch, "Calabi-Yau hypersurfaces in products of semi-ample surfaces," *Comm. Math. Phys.* **115** (1988) 231–246.

[23] D. R. Morrison and C. Vafa, "Compactifications of F theory on Calabi-Yau threefolds. 1," *Nucl. Phys. B* **473** (1996) 74–92.

[24] E. Witten, "Phase transitions in M theory and F theory," *Nucl. Phys.* **B471** (1996) 195–216.

[25] P. Berglund, T. Hübsch, and L. Parkes, "Gauge-neutral matter in a three-generation superstring compactification," *Mod. Phys. Lett.* **A5** (1990) 1485.

[26] P. Berglund, T. Hübsch, and L. Parkes, "The complete massless matter spectrum of a three-generation compactification," *Comm. Math. Phys.* **148** (1992) 57.

[27] J. Gray and J. Wang, "Jumping spectra and vanishing couplings in heterotic line bundle standard models," JHEP **11** (2019) 073.

[28] T. Wu and C. Yang *Phys. Rev. D* **12** (1975) 3845.

[29] P. Berglund, S. H. Katz, and A. Klemm, "Mirror symmetry and the moduli space for generic hypersurfaces in toric varieties," *Nucl. Phys.* **B456** (1995) 153–204.

[30] G. Kempf, F. Knudsen, D. Mumford, and B. Saint-Donat, *Toroidal Embeddings 1.* No. 339 in Lecture Notes in Mathematics. Springer, 1973.

[31] V. I. Danilov, "The geometry of toric varieties," *Russian Math. Surveys* **33** no. 2, (1978) 97–154.

[32] D. A. Cox, "The homogeneous coordinate ring of a toric variety," *J. Algebraic Geometry* **4** (1995) 17–50. Erratum: *J. Algebraic Geometry* **23** (2014) 393–398.

[33] P. S. Green and T. Hübsch, "Polynomial deformations and cohomology of Calabi-Yau manifolds," *Comm. Math. Phys.* **113** (1987) 505–528.

[34] N.-H. Lee, *Constructive Calabi-Yau Manifolds.* PhD thesis, University of Michigan, 2006.

[35] A. N. Tyurin, "Fano versus Calabi-Yau," in *The Fano Conference*, pp. 701–734. Univ. Torino, Turin, 2004.

[36] P. S. Green and T. Hübsch, "Connecting moduli spaces of Calabi-Yau threefolds," *Comm. Math. Phys.* **119** (1988) 431–441.

[37] P. Candelas, P. S. Green, and T. Hübsch, "Rolling among Calabi-Yau vacua," *Nucl. Phys.* **B330** (1990) 49–102.

[38] A. C. Avram, P. Candelas, D. Jancic, and M. Mandelberg, "On the connectedness of moduli spaces of Calabi-Yau manifolds," *Nucl. Phys.* **B465** (1996) 458–472.

[39] A. C. Avram, M. Kreuzer, M. Mandelberg, and H. Skarke, "The Web of Calabi-Yau hypersurfaces in toric varieties," *Nucl. Phys.* **B505** (1997) 625–640.

[40] C. F. Doran, A. Harder, and A. Thompson, "Mirror symmetry, Tyurin degenerations and fibrations on Calabi-Yau manifolds," *Proc. Symp. Pure Math.* **96** (2017) 93–131.

[41] A. Kanazawa, "Doran-Harder-Thompson conjecture via SYZ mirror symmetry: Elliptic curves," *Symmetry, Integrability and Geometry: Methods and Applications* **13** (Apr, 2017) 024.

[42] C. F. Doran, J. Kostiuk, and F. You, "The Doran-Harder-Thompson conjecture for toric complete intersections," Adv. Math. **415** (2023) 108893.

[43] C. F. Doran and A. Thompson, "Mirror symmetry for lattice polarized del pezzo surfaces," *Communications in Number Theory and Physics* **12** no. 3, (2018) 543–580.

[44] L. J. Barrott and C. F. Doran, "Towards the Doran-Harder-Thompson conjecture via the Gross-Siebert program," `arXiv:2105.02617 [math.AG]`.

[45] C. F. Doran and A. Thompson, "The mirror Clemens-Schmid sequence," `arXiv:2109.04849 [math.AG]`.

[46] C. F. Doran, J. Kostiuk, and F. You, "Degenerations, fibrations and higher rank Landau-Ginzburg models," `arXiv:2112.12891 [math.AG]`.

[47] M. Kreuzer and H. Skarke, "On the classification of quasihomogeneous functions," *Commun. Math. Phys.* **150** (1992) 137.

[48] M. Kreuzer and H. Skarke, "On the classification of reflexive polyhedra," *Commun. Math. Phys.* **185** (1997) 495–508.

[49] A. Hattori and M. Masuda, "Theory of multi-fans," *Osaka J. Math.* **40** (2003) 1–68.

[50] Y. Nishimura, "Multipolytopes and convex chains," *Proc. Steklov Inst. Math.* **252** (2006) 212–224.

[51] M. Kreuzer and H. Skarke, "Classification of reflexive polyhedra in three dimensions," *Adv. Theor. Math. Phys.* **2** no. 4, (1998) 853–871.

[52] Y. Karshon and S. Tolman, "The moment map and line bundles over presymplectic toric manifolds," *J. Diff. Geom.* **38** no. 3, (1993) 465–484.

[53] M. Kontsevich, "Homological algebra of mirror symmetry," in *Proceedings of the International Congress of Mathematicians*, S. D. Chatterji, ed., pp. 120–139. Birkhäuser Basel, Basel, 1995.

[54] A. Strominger, S.-T. Yau, and E. Zaslow, "Mirror symmetry is T-duality," *Nucl. Phys.* **B479** (1996) 243–259.

[55] C. Vafa, "String vacua and orbifoldized LG models," *Mod. Phys. Lett.* **A12** (1989) 1169–1185.

[56] K. A. Intriligator and C. Vafa, "Landau-Ginzburg orbifolds," *Nucl. Phys.* **B339** (1990) 95–120.

[57] M. Lynker and R. Schimmrigk, "Landau-Ginzburg theories as orbifolds," *Phys. Lett. B* **249** (1990) 237–242.

[58] P. Candelas, X. C. de la Ossa, P. S. Green, and L. Parkes, "A pair of Calabi-Yau manifolds as an exactly soluble superconformal theory," *Nucl. Phys.* **B359** (1991) 21–74.

[59] B. R. Greene and M. R. Plesser, "Mirror manifolds: A Brief review and progress report," in *2nd International Symposium on Particles, Strings and Cosmology.* 9, 1991.

[60] R. Schimmrigk, "Mirror symmetry in string theory and fractional transformations," in *2nd International Symposium on Particles, Strings and Cosmology (PASCOS 1991) Boston, MA*, pp. 681–695. March 25-30, 1991.

[61] R. Schimmrigk, "The construction of mirror symmetry," `arXiv: hep-th/9209018 [hep-th]`.

[62] M. Lynker and R. Schimmrigk, "Conifold transitions and mirror symmetries," *Nucl. Phys.* **B484** (1997) 562–582.

[63] M. Shoemaker, "Birationality of Berglund-Hübsch-Krawitz mirrors," *Comm. Math. Phys.* **331** (Oct., 2014) 417–429.

[64] T. L. Kelly, "Berglund-Hübsch-Krawitz mirrors via Shioda maps," *Adv. Theor. Math. Phys.* **17** no. 6, (2013) 1425–1449.

[65] P. Clarke, "A proof of the birationality of certain BHK-mirrors," *Complex Manifolds* **1** no. 1, (2013) 45–51.

[66] P. Clarke, "Birationality and Landau-Ginzburg models," *Comm. Math. Phys.* **353** no. 3, (2017) 1241–1260.

[67] F. Severi, "On the symbol of virtual intersection of algebraic varieties," in *Algebraic Geometry and Topology*, R. H. Fox, ed., vol. 1873 of *Princeton Legacy Library*, pp. 157–166. Princeton University Press, Princeton, NJ, 1957.

[68] S. J. Gates, Jr., M. T. Grisaru, M. Roček, and W. Siegel, *Superspace.* Benjamin/Cummings Pub. Co., Reading, MA, 1983.

[69] J. Wess and J. Bagger, *Supersymmetry and Supergravity.* Princeton Series in Physics. Princeton University Press, Princeton, NJ, 2nd ed., 1992.

[70] I. L. Buchbinder and S. M. Kuzenko, *Ideas and Methods of Supersymmetry and Supergravity.* Studies in High Energy Physics Cosmology and Gravitation. IOP Publishing Ltd., Bristol, 1998.

[71] T. Hübsch, "Haploid (2,2)-superfields in 2-dimensional space-time," *Nucl. Phys.* **B555** no. 3, (1999) 567–628.

[72] T. Hübsch, "Calabi-Yau manifolds — motivations and constructions," *Commun. Math. Phys.* **108** (1987) 291–318.

[73] P. Candelas, A. M. Dale, C. A. Lutken, and R. Schimmrigk, "Complete intersection Calabi-Yau manifolds," *Nucl. Phys.* **B298** (1988) 493.

[74] F. Kirwan and J. Woolf, *An Introduction to Intersection Homology Theory.* Chapman & Hall/CRC, 2006.

[75] M. Banagl, *Intersection Spaces, Spatial Homology Truncation, and String Theory.* No. 1997 in Lecture Notes in Mathematics. Springer, 2010.

[76] I. B. Frenkel, H. Garland, and G. J. Zuckerman, "Semiinfinite Cohomology and String Theory," *Proc. Nat. Acad. Sci.* **83** (1986) 8442.

[77] M. Atiyah and G. B. Segal, "On equivariant Euler characteristics," *J. Geom. Phys.* **6** no. 4, (1989) 671–677.

[78] V. V. Batyrev and L. A. Borisov, "Mirror duality and string-theoretic Hodge numbers," *Invent. Math.* **126** no. 1, (1996) 183–203.

[79] T. Hübsch, "On a stringy singular cohomology," *Mod. Phys. Lett.* **A12** (1997) 521–533.

[80] A. Rahman, "A perverse sheaf approach toward a cohomology theory for string theory," *Adv. Theor. Math. Phys.* **13** no. 3, (2009) 667–693.

[81] P. S. Aspinwall, T. Bridgeland, A. Craw, M. R. Douglas, A. Kapustin, G. W. Moore, M. Gross, G. Segal, B. Szendrői, and P. M. H. Wilson, *Dirichlet branes and mirror symmetry*, vol. 4 of *Clay Mathematics Monographs.* AMS, Providence, RI, 2009.

[82] R. J. Baston and M. G. Eastwood, *The Penrose Transform—Its Interaction with Representation Theory.* Claredon Press, Oxford, 1989.

[83] M. G. Eastwood and T. Hübsch, "Endomorphism valued cohomology and gauge singlet matter from superstrings," *Comm. Math. Phys.* **132** (1990) 383–413.

DEPARTMENT OF PHYSICS, UNIVERSITY OF NEW HAMPSHIRE
DURHAM, NH 03824, USA
E-mail address: `per.berglund@unh.edu`

DEPARTMENT OF PHYSICS & ASTRONOMY, HOWARD UNIVERSITY
WASHINGTON, DC 20059, USA
E-mail address: `thubsch@howard.edu`